J Stat Phys (2008) 130: 39–67
DOI 10.1007/s10955-007-9425-7

Chemomechanical Coupling of Molecular Motors: Thermodynamics, Network Representations, and Balance Conditions

Reinhard Lipowsky · Steffen Liepelt

Received: 21 July 2007 / Accepted: 4 September 2007 / Published online: 6 October 2007
© Springer Science+Business Media, LLC 2007

Abstract Molecular motors are considered that convert the chemical energy released from the hydrolysis of adenosine triphosphate (ATP) into mechanical work. Such a motor represents a small system that is coupled to a heat reservoir, a work reservoir, and particle reservoirs for ATP, adenosine diphosphate (ADP), and inorganic phosphate (P). The discrete state space of the motor is defined in terms of the chemical composition of its catalytic domains. Each motor state represents an ensemble of molecular conformations that are thermally equilibrated. The motor states together with the possible transitions between neighboring states define a network representation of the motor. The motor dynamics is described by a continuous-time Markov process (or master equation) on this network. The consistency between thermodynamics and network dynamics implies (i) local and nonlocal balance conditions for the transition rates of the motor and (ii) an underlying landscape of internal energies for the motor states. The local balance conditions can be interpreted in terms of constrained equilibria between neighboring motor states; the nonlocal balance conditions pinpoint chemical and/or mechanical nonequilibrium.

Keywords Energy transduction · Cytoskeletal motors · Stochastic processes · Entropy production

1 Introduction

Many molecular motors that one encounters in biological cells are powered by the hydrolysis of adenosine triphosphate. These motors represent ATPases, i.e., catalysts or enzymes for the hydrolysis of ATP. For the concentrations which prevail in living cells, the ATP hydrolysis is strongly exergonic or 'downhill' but it is also quite slow in the absence of any enzymatic activity. The motors act as enzymes for this chemical reaction and dramatically increase its reaction rate. In addition, these motors are also able to convert the chemical energy released from the ATP hydrolysis into useful work. In fact, this energy conversion occurs at the level

R. Lipowsky (✉) · S. Liepelt
Max-Planck-Institute of Colloids and Interfaces, Science Park Golm, 14424 Potsdam, Germany
e-mail: Reinhard.Lipowsky@mpikg-golm.mpg.de

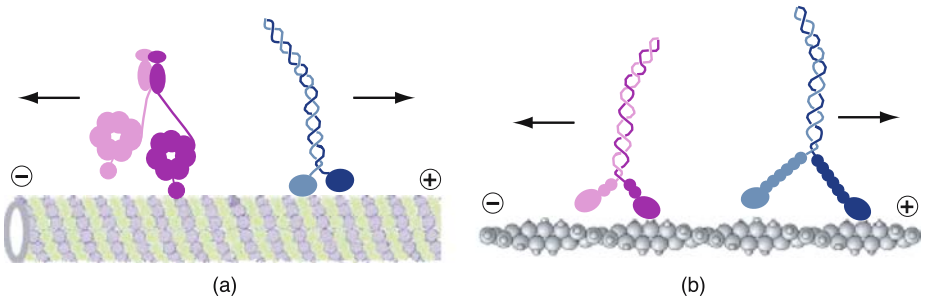

Fig. 1 Stepping motors that walk along cytoskeletal filaments, which are polar and have two different ends, a plus and a minus end: (**a**) Kinesin and dynein motor that move to the plus and minus end, respectively, of a microtubule; and (**b**) Myosin V and myosin VI that move to the plus (or barbed) and minus (or pointed) end, respectively, of an actin filament. The diameter of the microtubule and the actin filament are 25 nm and 8 nm, respectively. For simplicity, the cargo binding domains of the motors have been omitted. All four types of molecular motors are dimers consisting of two identical protein chains and use ATP hydrolysis in order to move in a directed manner. Kinesin and the two myosin motors walk in a 'hand-over-hand' fashion

of *single* hydrolysis events which implies that one should use a theoretical description that incorporates the discrete nature of these events.

In this article, we will consider molecular motors that are powered by ATP hydrolysis and have a certain fixed number of catalytic motor domains. Prominent examples are cytoskeletal motors such as kinesin, see Fig. 1(a), that are essential for intracellular transport, cell division, and cell locomotion [1, 2]. Three superfamilies of cytoskeletal motors have been identified: kinesins, dyneins and myosins [2, 3]. Kinesins and dyneins bind to microtubuli as shown in Fig. 1(a) whereas myosins bind to actin filaments as in Fig. 1(b).

Kinesin has two identical motor heads, each of which has a single catalytic domain for ATP hydrolysis. The same overall structure applies to processive myosins. Dyneins, on the other hand, have a more complex structure: they also have two motor heads as indicated in Fig. 1(a) but each head contains four ATP binding domains. One of these ATP binding domains appears to be the primary site for ATP hydrolysis, even though there is some evidence that the three other binding domains may also have some catalytic activity [4].

Kinesin and the other stepping motors transduce the chemical energy released from ATP hydrolysis into mechanical steps or displacements along the filament. Kinesin walks in a 'hand-over-hand' fashion, i.e., by alternating steps in which one head moves forward while the other one remains bound to the filament [5, 6]. Each step corresponds to a motor displacement of 8 nm corresponding to the lattice constant of the microtubule. It has also been found that these mechanical steps of kinesin are fast and completed within 15 microseconds [7]. This implies that there are no mechanical substeps on the time scales of the chemical transitions which take several milliseconds.

Kinesin exhibits tight coupling, i.e., it hydrolyzes one ATP molecule per mechanical step [8]. After ATP has been hydrolyzed by one of the catalytic motor domains, the inorganic phosphate is released rather fast, and both transitions together take of the order of 10 milliseconds to be completed [9]. ADP is subsequently released from the catalytic domain, and this release process is also completed during about 10 milliseconds [10]. When the catalytic domain of the motor head is occupied by ADP, this head is only loosely bound to the microtubule [11, 12] and most likely to unbind from it. Various motor properties such as motor velocity [7, 13], bound state diffusion coefficient (or randomness parameter) [13], ratio of forward to backward steps [7], and run length [14] were measured as a function of

ATP concentration and load force. Furthermore, the motor velocity was also determined as a function of P and ADP concentration [15].

We have recently developed a network theory for kinesin [16–18] that describes all of these experimental observations in a quantitative manner. The present article extends this previous work and has two related objectives: (i) To clarify the basic assumptions and the logical coherence of our theory; and (ii) To compare and contrast our approach with other theoretical studies.

Our theory has three basic ingredients: thermodynamics, network representations, and balance conditions. As far as thermodynamics is concerned, we explicitly consider all four thermodynamic control parameters, which govern a molecular motor at fixed temperature: the three chemical potentials of ATP, ADP, and P as well as the load force acting on the motor parallel to the filament. In this way, we avoid the limitations of previous studies [19–32] that explored only a certain subspace of this 4-dimensional space of thermodynamic control parameters.

In general, the external force as applied in single molecule experiments is a 3-dimensional vector with one component parallel to the filament, which defines the load force, and additional components, which act perpendicular to this filament. Since the motor does not perform mechanical work against the perpendicular force components, the latter components do *not* represent thermodynamic control parameters, even though they can affect the motor dynamics.

The second basic ingredient of our theory are network representations for molecular motors with M catalytic ATPase domains. These representations correspond to discrete state spaces in which the motor states are distinguished by the chemical composition of the catalytic domains. For $M = 1$, the state space has three motor states and corresponds to a reduced version of the ATPase model as previously considered by T.L. Hill [19] in the absence of mechanical work. For a motor with M domains, the state space consists of 3^M motor states. Starting from a certain state i, the motor can reach a number of neighboring states j via chemical or mechanical transitions $|ij\rangle$. The number of chemical transitions follows directly from the construction of the state space: each motor state is connected to $2M$ neighboring states via chemical transitions that correspond to the binding or unbinding of one of the chemical species. Kinesin has $M = 2$ catalytic domains and its basic network representation consists of 9 states and 36 chemical transitions. The number of mechanical transitions depends on the motor species. As mentioned, recent experiments on kinesin provide strong evidence [7] that this motor is governed by a single forward and backward step along the filament without any substeps.

For a single catalytic motor domain ($M = 1$), the network consists of a single dissipative cycle that transforms chemical energy into heat. This provides one example for a *slip* cycle that does *not* couple ATP hydrolysis to mechanical work. For $M \geq 2$, the networks contain many cycles including *chemomechanical* ones that convert chemical energy into work. As shown in [17], three different chemomechanical cycles have to be taken into account in order to understand the single molecule data on kinesin. In this way, our network theory differs from previous theories as described in [21–23, 26, 30–32] which were all based on a single chemomechanical motor cycle.

The third basic ingredient of our theory are balance conditions for the transitions between motor states which follow from the conservation of energy during these transitions. As in classical transition-state theory [33, 34] and in Kramers theory [35] for chemical kinetics [36, 37], we assume that each state of the motor molecule is internally equilibrated at a certain, fixed temperature. The same assumption was used in previous studies of energy transduction by molecular motors, see, e.g., [21, 38, 39]. However, in contrast to these

previous studies, we then focus on the internal energies of these states rather than on their free energies. Indeed, in our approach, the internal energy, U_i, is the most natural choice for the thermodynamic potential of the motor state i since its change is directly related to the first law of thermodynamics. Furthermore, within our theory, we can determine the internal energies of the motor states in terms of experimentally accessible quantities.

In order to proceed any further, we need to consider a specific model for the motor dynamics. The presumably simplest dynamics is provided by a continuous-time Markov process (or master equation) which depends on the rates ω_{ij} for the transitions $|ij\rangle$. For these Markov processes, one can calculate the entropies produced by the motor and, in this way, express the heat released by it in terms of the transition rates ω_{ij}. As a result, we obtain local and nonlocal energy balance relations which we reinterpret as balance *conditions* for the transition rates ω_{ij}.

The nonlocal conditions, which we first derived in [16], relate the transition rate ratios ω_{ij}/ω_{ji} for all transitions $|ij\rangle$ of a directed cycle (or dicycle) to the chemical energy change $\Delta\mu$ per ATP hydrolysis and to the load force F. The local conditions, which are consistent with the proposal of U. Seifert et al. [40, 41] about the entropy produced during a single transition, determine the dependence of the transition rates on the concentrations of ATP, ADP and P and strongly constrain the force dependence of these rates.

Our article is organized as follows. We start in Sect. 2 with the thermodynamics of the motor and the different reservoirs to which it is coupled. We then introduce our network representations in Sect. 3 where we start with the unicycle model of a single catalytic motor domain, describe the multi-cycle models for two-headed motors with two catalytic domains, and distinguish chemomechanical cycles from dissipative, mechanical, and thermal slip cycles. The elementary form of the energy balance relations is discussed in Sect. 4. The dynamics of the motor is then specified in Sect. 5 and the produced entropies are calculated in Sect. 6. If these entropies are identified with the heat released by the motor, the general energy balance relations of Sect. 4 lead to local and nonlocal balance conditions for the transition rates ω_{ij}, see Sect. 7. Finally, we calculate the landscape of internal energies in Sect. 8 and reinterpret the local and nonlocal balance conditions in Sect. 9.

2 Thermodynamics of Motor Plus Reservoirs

The molecular motor is taken to be embedded in a large amount of water and will be treated as a small system that is coupled to several reservoirs: (i) A heat reservoir at temperature T; (ii) A work reservoir characterized by the load force F; and (iii) Particle reservoirs for the chemical species $X =$ ATP, ADP, and inorganic phosphate P. These different types of reservoirs are displayed in Fig. 2.

We will always assume that the motor is in thermal equilibrium with its environment, i.e., the motor is always characterized by the same temperature T as the surrounding solution. Indeed, its internal vibrational modes are equilibrated by frequent, nonreactive collisions with a huge number of water molecules. Furthermore, the single motor is unlikely to perturb the Maxwell-Boltzmann velocity distribution of the water molecules in any substantial way. The same assumption of internal or local thermal equilibration underlies both classical transition-rate theory [33, 34] and Kramers theory [35] for chemical kinetics, as reviewed, e.g., in [36, 37].

Interaction of the molecular motor with the work reservoir is governed by the load force F. This force acts parallel to the filament and is taken to have a constant value independent of the spatial position of the motor. We use the convention that F is positive if it

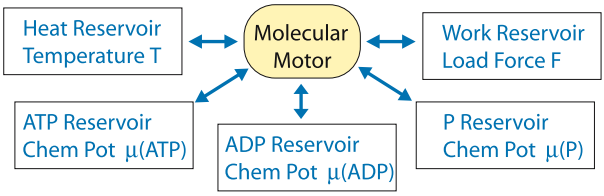

Fig. 2 Thermodynamic view of a molecular motor that is coupled to several reservoirs: A heat reservoir at temperature T; particle exchange reservoirs for ATP, ADP, and P with chemical potentials μ(ATP), μ(ADP), and μ(P); and a work reservoir governed by load force F. The motor is always taken to be in thermal equilibrium at temperature T but can be in chemical equilibrium or nonequilibrium depending on the size of the three chemical potentials. Mechanical equilibrium corresponds to $F = 0$

acts against the prefered movement of the motor. If the motor moves by the distance ℓ in its prefered direction along the filament, it performs the mechanical work

$$W_{\rm me} = \ell F > 0 \quad \text{for } F > 0. \tag{2.1}$$

Mechanical equilibrium between motor and work reservoir corresponds to $F = 0$. As mentioned in the introduction, the externally applied force is a 3-dimensional vector, which may have additional components that act perpendicular to the filament. It is convenient to choose Cartesian coordinates, (x, y, z), in such a way that the x-axis is parallel to the filament. The external force $\vec{F}_{\rm ex}$ then has the general form

$$\vec{F}_{\rm ex} = (F, \mathbf{F}_\perp) \quad \text{with } \mathbf{F}_\perp \equiv (F_{\perp y}, F_{\perp z}), \tag{2.2}$$

i.e., its x-component is equal to the load force F, and its y- and z-components define the 2-dimensional perpendicular force $\mathbf{F}_\perp$. The perpendicular force components do not represent thermodynamic control parameters, however, since the running motor bound to the filament does not perform mechanical work against $\mathbf{F}_\perp$. The possible influence of $\mathbf{F}_\perp$ on the motor dynamics will be considered in Sect. 7 below.

The exchange equilibria between the motor and the reservoirs for the chemical species $X =$ ATP, ADP, and P are governed by the corresponding chemical potentials, $\mu(X)$. The activity of X will be denoted by $[X]$ and is equal to the molar concentration in the limit of dilute solutions. In the following, we will use the term 'concentration' to be a synonym for 'activity'. For each activity $[X]$, we choose the activity scale $[X]^*$ in such a way that the chemical potential $\mu(X)$ has the simple form

$$\mu(X) = k_B T \ln([X]/[X]^*). \tag{2.3}$$

The activity scale $[X]^*$ can be determined theoretically using the grand-canonical ensemble. One then has to consider a large volume V of aqueous solution and calculate the partition functions Z_0 and Z_1 which correspond to the volume V containing either no or a single molecule of species X, respectively. The activity scale $[X]^*$ is then given by $[X]^* = Z_1/Z_0 V N_{\rm Av}$ with the Avogadro number $N_{\rm Av}$.

When the motor hydrolyzes a single ATP molecule, it binds one such molecule and releases one inorganic phosphate P and one ADP molecule. According to the Gibbs fundamental form of thermodynamics, the corresponding change in internal energy of the motor is given by

$$\Delta\mu = \mu(\text{ATP}) - \mu(\text{P}) - \mu(\text{ADP}) \tag{2.4}$$

which also represents the chemical energy input from the aqueous solution to the motor molecule. Using the expression (2.3) for the three chemical potentials, we then obtain

$$\Delta\mu = \ln\left(\frac{[\mathrm{ATP}]}{[\mathrm{ADP}][\mathrm{P}]}K^{\mathrm{eq}}\right) \quad \text{with } K^{\mathrm{eq}} \equiv \frac{[\mathrm{ADP}]^*[\mathrm{P}]^*}{[\mathrm{ATP}]^*} \tag{2.5}$$

which defines the equilibrium (dissociation) constant K^{eq}. Chemical equilibrium between ATP hydrolysis and ATP synthesis corresponds to $\Delta\mu = 0$ which implies

$$K^{\mathrm{eq}} = \left.\frac{[\mathrm{ADP}][\mathrm{P}]}{[\mathrm{ATP}]}\right|^{\mathrm{eq}}. \tag{2.6}$$

For dilute solutions, the activities of the three chemical species are equal to their molar concentrations and can be directly measured (after the system has relaxed into chemical equilibrium). For ATP hydrolysis, the precise value of the equilibrium constant K^{eq} depends on the ionic conditions but a typical value is given by $K^{\mathrm{eq}} = 4.9 \times 10^{11}$ μM [15, 42]. Thus, in thermal equilibrium at temperature T, a single molecular motor is governed by the 4-dimensional space of thermodynamic parameters, which can be defined in terms of the three activities or concentrations $[X]$ with $X =$ ATP, ADP, and P as well as the load force F or, equivalently, in terms of the three chemical potentials $\mu(X)$ and F.

Previous theoretical studies have explored certain subspaces of this 4-dimensional space of thermodynamic parameters. In his study of a generic ATPase, T.L. Hill [19] took all three concentrations into account but did not consider a load force. Hill emphasized that the chemical energy change $\Delta\mu$ per ATP hydrolysis as given by (2.4) acts as a 'thermodynamic force' that moves the system out of equilibrium. Several authors have subsequently focused on the 2-dimensional subspace as defined by this chemical energy change $\Delta\mu$ and the load force F [21, 22, 27, 31, 32]. A different 2-dimensional su bspace has been pursued in [20, 24, 25, 28, 29] in which the motor behavior was studied as a function of ATP concentration and load force. Furthermore, the theoretical studies in [23, 26, 30] focussed on the load force F and did not include the chemical coordinates involved in ATP hydrolysis. In contrast to these previous studies, our theory as introduced in [16, 17] and elucidated here explores the complete 4-dimensional space of thermodynamic control parameters.

3 Network Representations

For a given position at the filament, the molecular motor can attain many molecular conformations which differ in the chemical composition of their catalytic domains and in thermally excited vibrational modes. Since we want to describe the hydrolysis of single ATP molecules, we will use a *discrete* state space and focus on the different chemical compositions of the catalytic domains. From a mathematical point of view, the chemical composition of the catalytic domains provides an equivalence relation which divides the molecular configurations of the motor into equivalence classes.

3.1 State Space for Single Catalytic Motor Domain

We start with a single catalytic domain as shown in Fig. 3. Such a catalytic domain can be occupied by a single ATP molecule, by the combination ADP/P, by a single ADP molecule, or can be empty. In this way, each catalytic domain can attain 4 different states, as shown

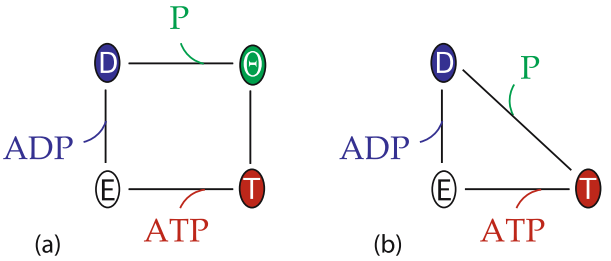

Fig. 3 Network representations for a single catalytic motor domain acting as an ATPase: (**a**) Network with 4 states corresponding to the catalytic domain being empty (E), occupied by ATP (T), by ADP/P (Θ), and by ADP (D); and (**b**) Reduced network with 3 states in which the hydrolysis transition and the P release transition have been combined into the single transition |TD⟩. As a result, each transition is now associated with the binding or release of a chemical species

in Fig. 3(a) where these states are represented as vertices in a network graph. Such a representation was previously used by T.L. Hill for a generic ATPase [19], see Appendix. The edges between the different chemical states in Fig. 3(a) represent forward and backward transitions. The edge between state i and state j will be denoted by $\langle ij \rangle$. It consists of two directed edges or di-edges, $|ij\rangle$ and $|ji\rangle$, corresponding to the forward transition from i to j and to the backward transition from j to i, respectively. Thus, the di-edge or transition |ET⟩ corresponds to ATP binding to the catalytic domain whereas the transition |TE⟩ represents ATP release from this domain. Likewise, the transitions |ΘD⟩, |DΘ⟩, |DE⟩, and |ED⟩ describe P release, P binding, ADP release, and ADP binding, respectively. Finally, the transition |TΘ⟩, corresponds to ATP hydrolysis proper and the transition |ΘT⟩ to ATP synthesis from ADP and P.

The three edges ⟨ET⟩, ⟨ΘD⟩, and ⟨DE⟩ involve the binding and release of a certain molecular species from the aqueous solution. In contrast, the edge ⟨TΘ⟩ in the 4-state network does not involve such an interaction of the catalytic domain with the particle reservoir, see Fig. 3(a). Therefore, one may combine the two edges ⟨TΘ⟩ and ⟨ΘD⟩ of the 4-state network into the edge ⟨TD⟩ as shown in Fig. 3(b). The latter representation involves only 3 states: the motor head is occupied by ADP in state D, empty in state E, and occupied by ATP in state T. This reduced representation is useful since it eliminates some parameters and can be defined in such a way that 3-state and 4-state network describe the same energy transduction process, see Appendix.

3.2 Two-Headed Motor with Two Catalytic Domains

Next, we consider a two-headed motor such as kinesin or myosin V with two identical catalytic motor domains. If each motor domain can attain three different chemical states as in Fig. 3(b), the two-headed motor can attain $3^2 = 9$ different states as in Fig. 4(a). In all of these states, the motor is bound to the filament. We use the convention that the right head is the leading head whereas the left head is the trailing head with respect to the prefered direction of the motor movement.

If the motor walks via the 'hand-over-hand' mechanism, the leading and the trailing head interchange their positions during each *mechanical* step. If one assumes that this step is fast on the timescale of the chemical transitions, one has, in general, three possible mechanical steps: from state (E, D) to state (D, E), from state (E, T) to state (T, E), and from state (D, T) to state (T, D). These possible mechanical transitions are shown in Fig. 4(a) as broken edges.

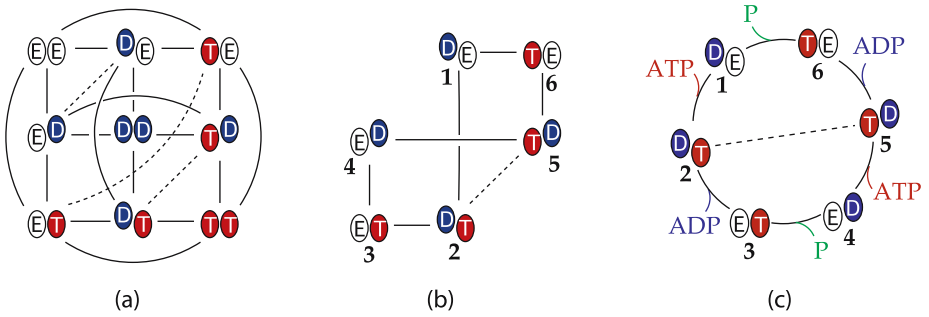

Fig. 4 Network representations for a molecular motor with two motor heads containing the same catalytic domain: Each head can be empty (E), occupied by ATP (T), or occupied by ADP (D): (**a**) State space with $3^2 = 9$ chemical states, each of which is connected to four neighboring states via *solid edges* (or *lines*). Each *solid edge* represents both the forward and backward chemical transition as in Fig. 3. Each *broken edge* (*or line*) represents both the forward and backward mechanical step transition in which the two heads interchange their relative position. We use the convention that the right and the left head correspond to the leading and trailing head, respectively; and (**b**), (**c**) Reduced state space with 6 chemical states, 6 *solid edges* representing chemical transitions, and one *broken edge* corresponding to the forward mechanical step from state 2 to state 5 and to the backward mechanical step from state 5 to state 2

Recent experiments by Carter and Cross [7] provide strong evidence that such a separation of time scales does indeed apply to the cytoskeletal motor kinesin.

Inspection of Fig. 4(a) shows that each state of the two-headed motor is connected to four other states via four solid edges. As in Fig. 3, each solid edge between two states i and j represents both the forward chemical transition $|ij\rangle$ and the backward transition $|ji\rangle$. Thus, each vertex of the 9-state network in Fig. 4(a) has 'chemical degree' four, and the whole network contains 18 solid edges corresponding to 36 *chemical* transitions. In addition, the 9-state network contains three possible mechanical transitions as indicated by the broken lines in Fig. 4(a).

As shown in [16, 17], the processive motion of kinesin is governed, to a large extent, by those motor states for which the two heads differ in their chemical composition. In addition, only one mechanical transition, namely from (D, T) to (T, D), is compatible with single motor data. The resulting 6-state network is shown in Fig. 4(b) and (c). The latter representation reveals that the six states form a cycle consisting of six (forward and backward) chemical transitions. The broken edge corresponds again to the mechanical step transition; according to our convention, the mechanical forward step is given by $|25\rangle$, the mechanical backward step by $|52\rangle$.

As shown in Fig. 4(c), the cycle of chemical transitions consists (i) of the two ATP binding transitions $|12\rangle$ and $|45\rangle$, (ii) of the two transitions $|61\rangle$ and $|34\rangle$, which both represent ATP hydrolysis and P release, as well as (iii) of the two ADP release transitions $|23\rangle$ and $|56\rangle$. The 'chemical degree' of all vertices in Fig. 4(c) is again equal to two, but the total vertex degree of the states $i = 2$ and $i = 5$ is equal to three because of the mechanical transition.

It is straightforward to generalize these considerations to a molecular motor with M catalytic domains. In this case, the different chemical compositions of the motor domains define 3^M motor states which are represented by 3^M vertices. Each of these vertices is connected to $2M$ other vertices via chemical transitions, i.e., each vertex has 'chemical degree' $2M$. As a result, one obtains a network with $M3^M$ chemical edges, each of which represents both a forward and a backward chemical transition.

3.3 Cycles and Dicycles

The two previous subsections provided two specific examples for the description of molecular motors in terms of a discrete state space. These states are represented as the vertices of a network graph, $\mathbb{G}$, and are labeled by $i = 1, 2, \ldots, |\mathbb{G}|$. Two neighboring states i and j are connected by an edge $\langle ij \rangle$ which represents the two di-edges or transitions $|ij\rangle$ and $|ji\rangle$. Inspection of Figs. 3 and 4 shows that these edges may form cycles. These cycles are particularly important in the present context since they are intimately related to fluxes and nonequilibrium states [19].

In order to be precise, we will distinguish (undirected) cycles from directed cycles or *dicycles*. The smallest dicycle consists of three states and three di-edges. An (undirected) cycle $\mathcal{C}_\nu$ is given by a closed sequence of neighboring vertices together with connecting edges, in which each vertex and each edge occurs only once. The notation $\mathcal{C}_\nu = \langle i_1 i_2 \ldots i_n i_1 \rangle$ implies that the cycle $\mathcal{C}_\nu$ contains the edges $\langle i_1 i_2 \rangle$, $\langle i_2 i_3 \rangle$, $\ldots$, and $\langle i_n i_1 \rangle$. Each cycle $\mathcal{C}_\nu$ leads to two dicycles $\mathcal{C}_\nu^d$ with $d = \pm$. First, we choose a certain arbitrary but fixed orientation of cycle $\mathcal{C}_\nu$ to correspond to the positive direction $d = +$, which defines the dicycle $\mathcal{C}_\nu^+$. When we pass through $\mathcal{C}_\nu$ in the opposite direction $d = -$, we obtain the dicycle $\mathcal{C}_\nu^-$. These two dicycles will be denoted by $\mathcal{C}_\nu^+ = |i_1 i_2 \ldots i_n i_1\rangle$ and $\mathcal{C}_\nu^- = |i_1 i_n \ldots i_2 i_1\rangle$.

The network description of a single motor head, see Fig. 3, involves only a single cycle. Analogous unicycle models have also been frequently used for two-headed motors, see, e.g., [26, 30]. Inspection of Fig. 4 shows, however, that these two-headed motors will, in general, exhibit several motor cycles. The 9-state network in Fig. 4(a) involves a rather large number of cycles (more than 200). In contrast, the 6-state network in Fig. 4(c) contains only three cycles: the forward cycle $\mathcal{F} = \langle 25612 \rangle$, the backward cycle $\mathcal{B} = \langle 52345 \rangle$, and the dissipative slip cycle $\mathcal{D} = \langle 1234561 \rangle$.

In order to distinguish different types of cycles, we will use the following terminology: (i) *Chemomechanical cycles* couple overall hydrolysis of ATP to a mechanical displacement of the motor and, in this way, are responsible for the energy transduction of the motor. Examples are given by the forward cycle $\mathcal{F} = \langle 25612 \rangle$ and the backward cycle $\mathcal{B} = \langle 52345 \rangle$ in the 6-state model, see Fig. 4(c); (ii) *Dissipative slip cycles* contain hydrolysis transitions but no mechanical step transition. Examples are provided by the cycles in the 4-state and 3-state networks of a single catalytic domain as shown in Fig. 3(a), and by the cycle $\mathcal{D} = \langle 1234561 \rangle$ of the 6-state model, see Fig. 4(c); (iii) *Mechanical slip cycles* contain mechanical step transitions but no net hydrolysis of ATP. Examples without any hydrolysis transitions are the cycles $\langle (\mathrm{E},\mathrm{E})(\mathrm{E},\mathrm{D})(\mathrm{D},\mathrm{E})(\mathrm{E},\mathrm{E}) \rangle$ and $\langle (\mathrm{E},\mathrm{T})(\mathrm{D},\mathrm{T})(\mathrm{T},\mathrm{D})(\mathrm{T},\mathrm{E})(\mathrm{E},\mathrm{T}) \rangle$ of the 9-state model, see Fig. 4(a). An example for a mechanical slip cycle with one ATP hydrolysis and one ATP synthesis transition is provided by the cycle $\langle (\mathrm{T},\mathrm{D})(\mathrm{D},\mathrm{D})(\mathrm{D},\mathrm{T})(\mathrm{T},\mathrm{D}) \rangle$; and (iv) *Thermal slip cycles* that involve neither a mechanical step nor a hydrolysis transition. Examples are provided by $\langle (\mathrm{E},\mathrm{E})(\mathrm{E},\mathrm{D})(\mathrm{D},\mathrm{D})(\mathrm{D},\mathrm{E})(\mathrm{E},\mathrm{E}) \rangle$ and $\langle (\mathrm{E},\mathrm{E})(\mathrm{E},\mathrm{T})(\mathrm{D},\mathrm{T})(\mathrm{D},\mathrm{E})(\mathrm{E},\mathrm{E}) \rangle$. It is interesting to note that the reduction of the 9-state model to the 6-state model eliminates all mechanical and thermal slip cycles from the network.

4 Internal Energies and Energy Transduction

We now assume that all vibrational modes or internal substates of motor state i are thermally equilibrated at temperature T. This assumption is based on a separation of time scales: thermal equilibration of single motor states is taken to be fast compared to the time that the motor needs to undergo the transitions between neighboring states. This separation of time

scales, which underlies both classical transition-rate theory and Kramers theory for chemical kinetics [33–37], is rather plausible for chemical reactions in liquids and has been previously emphasized in the context of discrete state models for molecular motors by T.L. Hill [38], and in the context of ratchet models by F. Jülicher et al. [21, 39].

4.1 Equilibration of Internal Substates

The substates of motor state i will be denoted by (i,k), the corresponding energies by $E_{i,k}$. The (conditional) probability $P_{i,k}$ to find the motor molecule in substate (i,k) then has the form

$$P_{i,k} = \frac{1}{Z_i} e^{-E_{i,k}/k_B T} \quad \text{with } Z_i \equiv \sum_k e^{-E_{i,k}/k_B T}. \tag{4.1}$$

The Helmholtz free energy, H_i, of the molecular motor state i is given by

$$H_i = -k_B T \ln(Z_i). \tag{4.2}$$

In his studies on biomolecules [19, 38, 43], T.L. Hill has considered this Helmholtz free energy H_i to be the 'basic free energy level' of such a biomolecular system. In contrast, we will focus here on the internal energy U_i of the motor state i since this thermodynamic potential enters the first law of thermodynamics. Thus, we will characterize each motor state i by its internal energy

$$U_i \equiv \langle E_{i,k} \rangle = \frac{1}{Z_i} \sum_k E_{i,k} e^{-E_{i,k}/k_B T}. \tag{4.3}$$

In general, we do not know the underlying energy spectrum $E_{i,k}$ and, thus, cannot calculate U_i via (4.3). However, we can express the internal energies U_i in terms of experimentally accessible quantities, see Sect. 8 below.

4.2 Energy Balance for Single Transitions

During the transition $|ij\rangle$ from state i to state j, the internal energy can change because of (i) chemical energy $\Delta\mu_{ij}$ arising from the coupling to the reservoirs for ATP, ADP, and P (ii) mechanical work $W_{\mathrm{me},ij}$, which the motor performs against the load force F, and (iii) heat Q_{ij}, which the motor releases into the surrounding medium. We use the convention that $Q_{ij} > 0$ if it increases the internal energy of the heat reservoir. Conservation of energy then implies the local energy balance relation [16]

$$\Delta U_{ij} \equiv U_j - U_i = \Delta\mu_{ij} - W_{\mathrm{me},ij} - Q_{ij} \tag{4.4}$$

for the transition $|ij\rangle$. If the chemical energy change $\Delta\mu_{ij}$ is positive, it may be partially *stored* in the motor molecule after the transition $|ij\rangle$, which implies $\Delta U_{ij} > 0$, and this stored energy may be transformed into work and/or heat during a later transition $|i'j'\rangle$, which implies $\Delta U_{i'j'} < 0$.

The chemical energy change $\Delta\mu_{ij}$ during the transition $|ij\rangle$ depends on the chemical potentials of the three chemical species $X =$ ATP, ADP, and P and is given by

$$\Delta\mu_{ij} = \begin{cases} 0 & \text{for no exchange during } |ij\rangle, \\ +\mu(X) & \text{for binding of X during } |ij\rangle, \\ -\mu(X) & \text{for release of X during } |ij\rangle \end{cases} \tag{4.5}$$

which implies $\Delta\mu_{ji} = -\Delta\mu_{ij}$.

The mechanical work $W_{\mathrm{me},ij}$ in the energy balance (4.4) depends on the mechanical displacement ℓ_{ij} during the transition $|ij\rangle$. Since the motor states i and j represent ensembles of molecular conformations, the quantity ℓ_{ij} should be viewed as a structural parameter of the system, the size of which is determined by the interaction between the motor and the filament. The corresponding mechanical work is given by

$$W_{\mathrm{me},ij} = \ell_{ij} F \tag{4.6}$$

where the load force $F > 0$ if it acts against the prefered direction of the motor ("resisting load"). Our sign convention for the load force and for the mechanical work W_{me} as given by (2.1) implies that $\ell_{ij} > 0$ and $\ell_{ij} < 0$ if the motor makes a mechanical forward and backward displacement, respectively.

4.3 Energy Balance for Dicycles

The energy balance relations simplify if we consider dicycles instead of single transitions. Indeed, if we sum the local energy balance as given by (4.4) over any dicycle $\mathcal{C}_\nu^d$, we obtain the dicycle relations

$$\sum_{|ij\rangle}^{\nu,d} [U_j - U_i] = \sum_{|ij\rangle}^{\nu,d} [\Delta\mu_{ij} - \ell_{ij} F - Q_{ij}] = 0 \tag{4.7}$$

where the superscript ν, d at the summation sign indicates that we sum over all di-edges or transitions $|ij\rangle$ of the dicycle $\mathcal{C}_\nu^d$.

The first term on the right hand side of the dicycle relation (4.7) can be expressed in terms of the overall chemical potential difference $\Delta\mu = \mu(\mathrm{ATP}) - \mu(\mathrm{ADP}) - \mu(\mathrm{P})$ as defined in (2.4). Indeed, inspection of the network models in Figs. 3 and 4 shows that each dicycle $\mathcal{C}_\nu^d$ can contain $n_{\mathrm{h}}(\mathcal{C}_\nu^d) \geq 0$ transitions that involve ATP hydrolysis and/or $n_{\mathrm{s}}(\mathcal{C}_\nu^d) \geq 0$ transitions that correspond to ATP synthesis. The chemical energy change per completed dicycle then has the explicit form

$$\Delta\mu(\mathcal{C}_\nu^d) \equiv \sum_{|ij\rangle}^{\nu,d} \Delta\mu_{ij} = [n_{\mathrm{h}}(\mathcal{C}_\nu^d) - n_{\mathrm{s}}(\mathcal{C}_\nu^d)]\Delta\mu \tag{4.8}$$

where $\Delta\mu$ can be expressed in terms of the activities $[X]$ and the equilibrium constant K^{eq} via (2.5). The quantity $\Delta\mu(\mathcal{C}_\nu^d)$ satisfies $\Delta\mu(\mathcal{C}_\nu^-) = -\Delta\mu(\mathcal{C}_\nu^+)$ and can be used to define *chemical* equilibrium and nonequilibrium for each cycle of the network: a certain cycle C_n is in chemical equilibrium and nonequilibrium if $\Delta\mu(\mathcal{C}_n^d) = 0$ and $\Delta\mu(\mathcal{C}_n^d) \neq 0$, respectively.

Furthermore, the second term on the right hand side of the dicycle energy balance (4.7) can be rewritten as

$$W_{\mathrm{me}}(\mathcal{C}_\nu^d) \equiv \sum_{|ij\rangle}^{\nu,d} \ell_{ij} F \equiv \ell(\mathcal{C}_\nu^d) F \tag{4.9}$$

which defines the mechanical displacement $\ell(\mathcal{C}_\nu^d)$ during the completed dicycle $\mathcal{C}_\nu^d$. For kinesin, which makes no mechanical substeps [7], $\ell(\mathcal{C}_\nu^d)$ is equal to 8 nm, the lattice parameter of microtubules. The quantity $W_{\mathrm{me}}(\mathcal{C}_\nu^d)$ satisfies $W_{\mathrm{me}}(\mathcal{C}_\nu^-) = -W_{\mathrm{me}}(\mathcal{C}_\nu^+)$ and can be used to define *mechanical* equilibrium and nonequilibrium for each cycle of the network: a certain cycle C_n is in mechanical equilibrium and nonequilibrium if $W_{\mathrm{me}}(\mathcal{C}_n^d) = 0$ and $W_{\mathrm{me}}(\mathcal{C}_n^d) \neq 0$, respectively.

Inserting the expressions (4.8) and (4.9) into the relation (4.7), we arrive at the dicycle balance relation [16]

$$Q(\mathcal{C}_\nu^d) \equiv \sum_{|ij\rangle}^{\nu,d} Q_{ij} = [n_{\mathrm{h}}(\mathcal{C}_\nu^d) - n_{\mathrm{s}}(\mathcal{C}_\nu^d)]\Delta\mu - \ell(\mathcal{C}_\nu^d)F \tag{4.10}$$

for the heat exchange $Q(\mathcal{C}_\nu^d)$ per completed dicycle $\mathcal{C}_\nu^d$.

5 Motor Dynamics

In order to proceed any further, we must now consider a specific model for the motor dynamics. The presumably simplest dynamics is provided by a continuous-time Markov process [37, 44] on the network graph $\mathbb{G}$. Such a process involves two stochastic ingredients, the sojourn (or dwell) times and the transition probabilities. When the system arrives in state i, it occupies this state for a certain sojourn (or dwell) time τ_i. This time is a random variable governed by the exponential probability distribution

$$P(\tau_i) = \frac{1}{\langle\tau_i\rangle} e^{-\tau_i/\langle\tau_i\rangle} \tag{5.1}$$

where $\langle\tau_i\rangle$ denotes the average sojourn time [44]. When the motor leaves the state i, it jumps to state j with transition probability π_{ij}. By definition, one has $\pi_{ii} \equiv 0$ for all i and $\sum_j \pi_{ij} = 1$. From the mathematical point of view, the latter transitions occur instantaneously; from the physical point of view, they occur on a time scale that is small compared to all average sojourn times $\langle\tau_i\rangle$.

The probability $P_i(t)$ to find the motor in state i at time t is then governed by the loss-and-gain equation

$$\frac{d}{dt} P_i = -\sum_j (P_i\omega_{ij} - P_j\omega_{ji}) \tag{5.2}$$

with the transition rates

$$\omega_{ij} = \pi_{ij}/\langle\tau_i\rangle \quad \text{and} \quad \sum_j \omega_{ij} = 1/\langle\tau_i\rangle. \tag{5.3}$$

In the physical literature, this equation is known as the master equation [37]; in the mathematical literature, it is called the forward equation of the continuous-time Markov process [44]. It is convenient to define the local fluxes (or currents) $J_{ij} \equiv P_i\omega_{ij}$ and the local excess fluxes

$$\Delta J_{ij} \equiv P_i\omega_{ij} - P_j\omega_{ji} = -\Delta J_{ji} \tag{5.4}$$

from state i to state j. The master equation (5.2) can then be rewritten in the compact form $\frac{d}{dt} P_i = -\sum_j \Delta J_{ij}$.

If the motor system is in full equilibrium, i.e., in thermal, chemical, and mechanical equilibrium, it is characterized by time-independent probabilities $P_i = P_i^{\mathrm{eq}}$ and local excess fluxes $\Delta J_{ij}^{\mathrm{eq}} = 0$ for all transitions $|ij\rangle$. In such a situation, the transition rates ω_{ij} must satisfy the detailed balance conditions

$$P_i^{\mathrm{eq}}\omega_{ij} = P_j^{\mathrm{eq}}\omega_{ji} \tag{5.5}$$

for all edges $\langle ij\rangle$ of the network graph.

The detailed balance conditions (5.5) can be expressed in terms of the transition rates ω_{ij} alone. In order to do so, it is convenient to define, for each dicycle $\mathcal{C}_\nu^d$, the *dicycle ratio*

$$\Xi(\mathcal{C}_\nu^d) \equiv \prod_{|ij\rangle\in\mathcal{C}_\nu^d} \omega_{ij} \Big/ \prod_{|ij\rangle\in\mathcal{C}_\nu^{-d}} \omega_{ij} = \prod_{|ij\rangle}^{\nu,d} (\omega_{ij}/\omega_{ji}) \tag{5.6}$$

where the superscript ν, d at the product sign indicates a product over all di-edges $|ij\rangle$ of the dicycle $\mathcal{C}_\nu^d$. This definition implies $\Xi(\mathcal{C}_\nu^-) = 1/\Xi(\mathcal{C}_\nu^+)$. The detailed balance conditions as given by (5.5) are equivalent to the dicycle ratios

$$\Xi^{\rm eq}(\mathcal{C}_\nu^d) = \prod_{|ij\rangle}^{\nu,d} (\omega_{ij}/\omega_{ji}) = 1 \quad \text{for all dicycles } \mathcal{C}_\nu^d, \tag{5.7}$$

as shown, e.g., in [29].

In general, the *steady state* of the motor system corresponds to $dP_i/dt = 0$ and leads to time-independent probabilities $P_i = P_i^{\rm st}$ which satisfy

$$\sum_j (P_i^{\rm st}\omega_{ij} - P_j^{\rm st}\omega_{ji}) = \sum_j \Delta J_{ij}^{\rm st} = \sum_j (J_{ij}^{\rm st} - J_{ji}^{\rm st}) = 0. \tag{5.8}$$

These relations represent $N_{\rm s}$ linear equations for the probabilities $P_i^{\rm st}$ which can be solved by linear algebra, see, e.g., [25, 28] or, more conveniently, by a graph-theoretic method [29, 45–48]. In the steady state, the motor undergoes the transition $|ij\rangle$ with the transition frequency

$$\Omega_{ij}^{\rm st} \equiv P_i^{\rm st}\omega_{ij}. \tag{5.9}$$

Likewise, one may define the dicycle frequency $\Omega^{\rm st}(\mathcal{C}_\nu^d)$, i.e., the number of completed di-cycles $\mathcal{C}_\nu^d$ per unit time in the steady state. As shown in [16, 49, 50], for a given cycle $\mathcal{C}_\nu$, the dicycle frequencies satisfy

$$\Omega^{\rm st}(\mathcal{C}_\nu^+)/\Omega^{\rm st}(\mathcal{C}_\nu^-) = \prod_{|ij\rangle}^{\nu,d} (\omega_{ij}/\omega_{ji}) = \Xi(\mathcal{C}_\nu^+) \tag{5.10}$$

which provides an intuitive interpretation of the dicycle ratio $\Xi(\mathcal{C}_\nu^+)$.

6 Entropy Production and Heat Exchange

We will now use the dynamics defined in the previous section in order to determine the entropy produced by the motor. The produced entropy will then be identified with the released heat which leads to energy balance equations between the transition rates ω_{ij} of the motor model and the thermodynamic control parameters.

6.1 Time Evolution of Statistical Entropy

We start from the statistical or Shannon entropy

$$S\{P_i\} \equiv -k_B \sum_i P_i \ln(P_i) \tag{6.1}$$

which one may define for any probability distribution $\{P_i\}$ on a discrete state space $\mathbb{G}$. This entropy provides a well-defined measure by which one can compare different probability distributions. If the probability distribution changes with time t, so does the statistical entropy $S\{P_i\}$. Its time derivative can be written in the form [48, 51–53]

$$\frac{d}{dt}S\{P_i\} = \sigma_{\rm pr}\{P_i\} + \sigma_{\rm fl}\{P_i\} \tag{6.2}$$

with the entropy production rate

$$\sigma_{\rm pr}\{P_i\} \equiv \frac{1}{2}k_B \sum_i {\sum_j}' (P_i\omega_{ij} - P_j\omega_{ji}) \ln\left(\frac{P_i\omega_{ij}}{P_j\omega_{ji}}\right) \tag{6.3}$$

and the entropy flux term

$$\sigma_{\rm fl}\{P_i\} \equiv -\frac{1}{2}k_B \sum_i {\sum_j}' (P_i\omega_{ij} - P_j\omega_{ji}) \ln\left(\frac{\omega_{ij}}{\omega_{ji}}\right) \tag{6.4}$$

where the prime at the summation sign indicates that there are no terms with $j = i$. Thus, the double sum represents a summation over all di-edges or transitions $|ij\rangle$ of the network.

Each term in the expression (6.3) for the entropy production rate has the form $(x - y)\ln(x/y)$ with $(x - y)\ln(x/y) > 0$ for $x \neq y$ and $(x - y)\ln(x/y) = 0$ for $x = y$. This implies that the entropy production rate $\sigma_{\rm pr}$ as given by (6.3) satisfies $\sigma_{\rm pr}\{P_i\} \geq 0$ for any distribution $\{P_i\}$ and vanishes if and only if $\{P_i\} = \{P_i^{\rm eq}\}$. These two properties characterize the entropy production rate in general, see, e.g., [54].

In the steady state, the system's entropy does not change and $\frac{d}{dt}S\{P_i\} = 0$, which implies

$$\sigma_{\rm pr}^{\rm st} \equiv \sigma_{\rm pr}\{P_i^{\rm st}\} = -\sigma_{\rm fl}\{P_i^{\rm st}\} \tag{6.5}$$

or

$$\sigma_{\rm pr}^{\rm st} = \frac{1}{2}\sum_i {\sum_j}' (P_i^{\rm st}\omega_{ij} - P_j^{\rm st}\omega_{ji})k_B \ln(\omega_{ij}/\omega_{ji}). \tag{6.6}$$

6.2 Entropy Production during Dicycle Completion

The expression (6.6) for the entropy production rate can be rewritten in the form [16]

$$\sigma_{\rm pr}^{\rm st} = \sum_\nu \sum_{d=\pm} \Omega^{\rm st}(\mathcal{C}_\nu^d)\Delta S(\mathcal{C}_\nu^d) \tag{6.7}$$

where the sum includes all dicycles of the network, $\Omega^{\rm st}(\mathcal{C}_\nu^d)$ denotes the dicycle frequency, i.e., the number of times this dicycle is completed per unit time, compare (5.10), and $\Delta S(\mathcal{C}_\nu^d)$ the entropy produced during completion of dicycle $\mathcal{C}_\nu^d$. The latter quantity is given by [16]

$$\Delta S(\mathcal{C}_\nu^d) = k_B \ln(\Xi(\mathcal{C}_\nu^d)) = k_B \ln\left(\prod_{|ij\rangle}^{\nu,d} (\omega_{ij}/\omega_{ji})\right) \tag{6.8}$$

where the definition (5.6) of the dicycle ratio $\Xi(\mathcal{C}_\nu^d)$ has been used. Since $\Xi(\mathcal{C}_\nu^-) = 1/\Xi(\mathcal{C}_\nu^+)$, the entropies of the two dicycles $\mathcal{C}_\nu^+$ and $\mathcal{C}_\nu^-$ are related via $\Delta S(\mathcal{C}_\nu^-) = -\Delta S(\mathcal{C}_\nu^+)$ which reflects the fact that the dicycle $\mathcal{C}_\nu^-$ corresponds to the time-reversed dicycle $\mathcal{C}_\nu^+$.

T.L. Hill and coworkers [19, 43] have previously discussed the quantity $k_B T$ times $\ln(\Xi(\mathcal{C}_\nu^d))$, which they viewed as the 'thermodynamic force' that drives the system out of equilibrium. Our work shows that this thermodynamic force is, in fact, equal to temperature T times dicycle entropy $\Delta S(\mathcal{C}_\nu^d)$.

Since the motor is in thermal equilibrium with the heat reservoir at temperature T, we identify T times the entropy $\Delta S(\mathcal{C}_\nu^d)$ produced during the dicycle $\mathcal{C}_\nu^d$ with the heat $Q(\mathcal{C}_\nu^d)$ released during this dicycle. The energy balance relation (4.10) then becomes

$$k_B T \ln[\Xi(\mathcal{C}_\nu^d)] = Q(\mathcal{C}_\nu^d) = [n_{\rm h}(\mathcal{C}_\nu^d) - n_{\rm s}(\mathcal{C}_\nu^d)]\Delta\mu - \ell(\mathcal{C}_\nu^d)F \tag{6.9}$$

or

$$k_B T \sum_{|ij\rangle}^{\nu,d} \ln\left(\frac{\omega_{ij}}{\omega_{ji}}\right) = [n_{\rm h}(\mathcal{C}_\nu^d) - n_{\rm s}(\mathcal{C}_\nu^d)]\Delta\mu - \ell(\mathcal{C}_\nu^d)F \tag{6.10}$$

which provides a relation between the transition rates ω_{ij} and the thermodynamic parameters of the motor system. In full equilibrium, one has $\Delta\mu = 0$ and $F = 0$, and we recover the detailed balance conditions with the dicycle ratio $\Xi(\mathcal{C}_\nu^d) = 1$ as in (5.7).

It is interesting to note that one may combine the relations (5.10) and (6.8) in order to express the dicycle frequency ratio $\Omega^{\rm st}(\mathcal{C}_\nu^+)/\Omega^{\rm st}(\mathcal{C}_\nu^-)$ in terms of the dicycle entropies via

$$\frac{\Omega^{\rm st}(\mathcal{C}_\nu^+)}{\Omega^{\rm st}(\mathcal{C}_\nu^-)} = e^{\Delta S(\mathcal{C}_\nu^+)/k_B} = e^{-\Delta S(\mathcal{C}_\nu^-)/k_B} \tag{6.11}$$

which is reminiscent of the various relations that have been derived in the context of entropy fluctuations [40, 55–57]. The entropies $\Delta S(\mathcal{C}_\nu^d)$ as considered here do not fluctuate, however, but have a certain, fixed value for each dicycle of the network.

6.3 Entropy Production during Single Transition

The entropy production rate as given by (6.6) and (6.7) can also be rewritten in the form

$$\sigma_{\rm pr}^{\rm st} = \sum_{|ij\rangle} P_i^{\rm st}\omega_{ij}\Delta S_{ij} = \sum_{|ij\rangle} \Omega_{ij}^{\rm st}\Delta S_{ij} \tag{6.12}$$

with the transition frequencies $\Omega_{ij}^{\rm st}$ as in (5.9) where the summation runs over all di-edges or transitions $|ij\rangle$ of the network. The transition entropies ΔS_{ij} are defined by [40]

$$\Delta S_{ij} \equiv k_B \ln(\omega_{ij}/\omega_{ji}) = -\Delta S_{ji}. \tag{6.13}$$

This definition of the transition entropies is consistent with the dicycle entropies as given by (6.8) since

$$\sum_{|ij\rangle}^{\nu,d} \Delta S_{ij} = \Delta S(\mathcal{C}_\nu^d) \tag{6.14}$$

for any dicycle $\mathcal{C}_\nu^d$ of the network.

If we now identify the transition entropy ΔS_{ij} times temperature T with the heat exchange Q_{ij}, the local energy balance relation (4.4) becomes

$$\Delta U_{ij} = U_j - U_i = \Delta\mu_{ij} - \ell_{ij}F - k_B T \ln(\omega_{ij}/\omega_{ji}). \tag{6.15}$$

This relation will be used further below in order to calculate the internal energies U_i and the equilibrium distribution $P_i^{\rm eq}$ for full equilibrium.

7 Local and Nonlocal Balance Conditions

We will now change our point of view and interpret the relations (6.10) and (6.15) as balance *conditions* that one has to *impose* on the transition rates ω_{ij} in order to obtain a dynamic or kinetic model that is consistent with thermodynamics. Since these conditions must apply, in particular, to the steady state of the system, we called them 'steady state balance conditions' in our previous work [16, 17].

7.1 Nonlocal Balance Conditions for Dicycles

First, we will show that the energy balance relations (6.10) and (6.15) strongly affect the functional dependence of the transition rates ω_{ij} on the activities $[X]$ and on the load force F. As explained in Sect. 2, the load force F acts parallel to the filament, and the externally applied force has the general form $\vec{F}_{\mathrm{ex}} = (F, \mathbf{F}_\perp)$ as in (2.2) with the 2-dimensional force $\mathbf{F}_\perp \equiv (F_{\perp y}, F_{\perp z})$ acting perpendicular to the filament. This perpendicular force may affect the transition rates ω_{ij} if the strain arising from $\mathbf{F}_\perp$ is sufficiently strong to deform the motor's molecular structure.

We now consider transition rates $\omega_{ij} = \omega_{ij}(F, \mathbf{F}_\perp)$ with arbitrary F- and $\mathbf{F}_\perp$-dependencies and decompose these rates according to

$$\omega_{ij}(F, \mathbf{F}_\perp) \equiv \omega_{ij,0} \Phi_{ij}(F) \zeta_{ij}(F, \mathbf{F}_\perp) \tag{7.1}$$

with the zero-force factor

$$\omega_{ij,0} \equiv \omega_{ij}(F = 0, \mathbf{F}_\perp = \mathbf{0}), \tag{7.2}$$

the load-dependent factor

$$\Phi_{ij}(F) \equiv \omega_{ij}(F, \mathbf{F}_\perp = \mathbf{0})/\omega_{ij,0} \quad \text{with } \Phi_{ij}(0) = 1, \tag{7.3}$$

and the additional factor

$$\zeta_{ij}(F, \mathbf{F}_\perp) \equiv \omega_{ij}(F, \mathbf{F}_\perp)/\omega_{ij}(F, \mathbf{F}_\perp = \mathbf{0}) \quad \text{with } \zeta_{ij}(F, \mathbf{0}) = 1 \tag{7.4}$$

which depends on the perpendicular force $\mathbf{F}_\perp$. This parametrization generalizes the one used in [16, 17] where we ignored possible perpendicular force components.

When we insert the parametrization (7.1) of the transition rates into the dicycle ratio $\Xi(\mathcal{C}_\nu^d)$ as defined by (5.6), the dicycle ratio factorizes according to

$$\Xi(\mathcal{C}_\nu^d) = \Xi_0(\mathcal{C}_\nu^d) \Xi_F(\mathcal{C}_\nu^d) \Xi_\perp(\mathcal{C}_\nu^d) \tag{7.5}$$

with the zero-force dicycle ratio

$$\Xi_0(\mathcal{C}_\nu^d) \equiv \prod_{|ij\rangle}^{\nu,d} \omega_{ij,0}/\omega_{ji,0}, \tag{7.6}$$

the load-dependent factor

$$\Xi_F(\mathcal{C}_\nu^d) \equiv \prod_{|ij\rangle}^{\nu,d} \Phi_{ij}(F)/\Phi_{ji}(F), \tag{7.7}$$

and

$$\Xi_\perp(\mathcal{C}_\nu^d) \equiv \prod_{|ij\rangle}^{\nu,d} \zeta_{ij}(F,\mathbf{F}_\perp)/\zeta_{ji}(F,\mathbf{F}_\perp). \tag{7.8}$$

Furthermore, when this factorized form of the dicycle ratio is inserted into the dicycle balance relation (6.10), this relation is decomposed into three parts. For $F=0$ and $\mathbf{F}_\perp=\mathbf{0}$, we obtain [16]

$$k_BT\ln[\Xi_0(\mathcal{C}_\nu^d)] = \Delta\mu(\mathcal{C}_\nu^d) = [n_{\rm h}(\mathcal{C}_\nu^d) - n_{\rm s}(\mathcal{C}_\nu^d)]\Delta\mu \tag{7.9}$$

which represents a balance condition for the zero-force transition rates $\omega_{ij,0}$ in terms of the chemical energy change $\Delta\mu$ per hydrolyzed ATP molecule. For $F\neq 0$ but $\mathbf{F}_\perp=\mathbf{0}$, the dicycle balance relation leads to the load-dependent balance condition [16]

$$k_BT\ln[\Xi_F(\mathcal{C}_\nu^d)] = -W_{\rm me}(\mathcal{C}_\nu^d) = -\ell(\mathcal{C}_\nu^d)F \tag{7.10}$$

which constrains the transition rate factors $\Phi_{ij}(F)$ in terms of the load force F. Finally, for $\mathbf{F}_\perp\neq\mathbf{0}$, the dicycle balance condition (6.10) implies

$$k_BT\ln[\Xi_\perp(\mathcal{C}_\nu^d)] = 0 \tag{7.11}$$

which represents a constraint on the additional force-dependent factors $\zeta_{ij}(F,\mathbf{F}_\perp)$.

7.2 Local Balance Conditions for Single Transitions

Using the transition rate parametrization (7.1), the local energy balance relation (6.15) becomes

$$U_j - U_i = \Delta\mu_{ij} - k_BT\ln\left(\frac{\omega_{ij,0}}{\omega_{ji,0}}\right) - \ell_{ij}F - k_BT\ln\left(\frac{\Phi_{ij}\zeta_{ij}}{\Phi_{ji}\zeta_{ji}}\right). \tag{7.12}$$

We now request that the internal energies U_i (i) must not depend on the activities $[X]$ and (ii) must be independent of both the load force F and the perpendicular force component $F_\perp$. The latter requirement implies

$$\Phi_{ij}(F)/\Phi_{ji}(F) = e^{-\ell_{ij}F/k_BT} \tag{7.13}$$

and

$$\zeta_{ij}(F,\mathbf{F}_\perp) = \zeta_{ji}(F,\mathbf{F}_\perp). \tag{7.14}$$

For the network models shown in Figs. 3 and 4, most of the transitions $|ij\rangle$ correspond to chemical transitions without any mechanical step which implies $\ell_{ij}=0$. In this case, the balance condition (7.13) for the load-dependent factors further simplifies and becomes

$$\Phi_{ij}(F) = \Phi_{ji}(F) \quad \text{for } \ell_{ij}=0. \tag{7.15}$$

This relation provides a direct justification for the load-dependent transition rate factors $\Phi_{ij}(F)$ as chosen in our previous study about kinesin [17]. In this latter case, we imposed the dicycle condition (7.10) on the transition rates and made the choice (7.15) since it was the simplest one that is compatible with this dicycle condition.

It is important to note that the absence of a partial mechanical step during the transition $|ij\rangle$, i.e., $\ell_{ij}=0$, does *not* imply that the transition rate ω_{ij} is independent of force.

It only implies that the load-dependent factor $\Phi_{ij}(F)$ and the additional factor $\zeta_{ij}(F, \mathbf{F}_\perp)$ of the transition rate ω_{ij} are equal to the corresponding factors $\Phi_{ji}(F)$ and $\zeta_{ji}(F, \mathbf{F}_\perp)$ of the rate ω_{ji} for the reverse transition.

The requirement (i) that the internal energies must not depend on any activity $[X]$ implies that the combination $\exp[\Delta\mu_{ij}/k_BT]\omega_{ji,0}/\omega_{ij,0}$ is independent of $[X]$. The definition (4.5) of $\Delta\mu_{ij}$ together with the chemical potentials $\mu(X) = k_BT\ln([X]/[X]^*)$ as in (2.3) then leads to the conclusion that

$$\omega_{ij,0} \propto \begin{cases} [X]\omega_{ji,0} & \text{for binding of X during } |ij\rangle, \\ \omega_{ji,0}/[X] & \text{for release of X during } |ij\rangle, \end{cases} \tag{7.16}$$

and that $\omega_{ij,0}$ is independent of all $[X]$ if the transition $|ij\rangle$ does not involve the binding or release of any chemical species. Since the release of species X during $|ij\rangle$ implies the binding of X during $|ji\rangle$, the two relations in (7.16) are, in fact, equivalent.

The release of species X from a catalytic motor domain is a thermally activated process and should not depend on the activity $[X]$ in the particle reservoir (provided the binding of the chemical species X to one catalytic motor domain does not induce the release of X from another catalytic domain). Therefore, the zero-force transition rate $\omega_{ij,0}$ for the release of X should be independent of $[X]$. Together with the balance relation (7.16), we then obtain the simple parametrizations

$$\omega_{ij,0} = \begin{cases} \kappa_{ij} & \text{for release of X during } |ij\rangle, \\ \kappa_{ij}[X] & \text{for binding of X during } |ij\rangle \end{cases} \tag{7.17}$$

which defines the $[X]$-independent transition rate constants κ_{ij}. The $[X]$-dependence of the zero-rate transition rates $\omega_{ij,0}$ as given by (7.17) is precisely what one would have chosen for physical adsorption of species $[X]$ to the molecular motor without use of the local energy balance conditions [17].

8 Energy Landscape of Internal Energies

We will now express the internal energies U_i in terms of the other model parameters. First, the balance conditions (7.13) and (7.14) for the force-dependent factors of the transition rates imply that the local energy balance condition (7.12) attains the simpler form

$$U_j - U_i = \Delta\mu_{ij} - k_BT\ln\left(\frac{\omega_{ij,0}}{\omega_{ji,0}}\right). \tag{8.1}$$

Second, using the definition (4.5) of $\Delta\mu_{ij}$ and the parametrization (7.17) of the zero-force transition rates $\omega_{ij,0}$, we finally obtain the internal energy differences

$$\Delta U_{ij} = U_j - U_i = -k_BT\ln\left(\frac{[X]^*\kappa_{ij}}{\kappa_{ji}}\right) \tag{8.2}$$

for binding of the chemical species X during the transition $|ij\rangle$,

$$\Delta U_{ij} = U_j - U_i = -k_BT\ln\left(\frac{\kappa_{ij}}{[X]^*\kappa_{ji}}\right) \tag{8.3}$$

for release of the chemical species X during the transition $|ij\rangle$, and

$$\Delta U_{ij} = U_j - U_i = -k_B T \ln\left(\frac{\kappa_{ij}}{\kappa_{ji}}\right) \tag{8.4}$$

if the transition $|ij\rangle$ does not involve any exchange with the particle reservoirs where $[X]^*$ is again the activity scale as in (2.3). The internal energy differences ΔU_{ij} as given by (8.2–8.4) determine the internal energies U_i of all motor states i up to an additive constant, say U_o. It is convenient to choose this constant U_o in such a way that the internal energy of a certain reference state $i = a$ is identically zero. In this way, we obtain the complete energy landscape underlying the Markovian motor dynamics. As a consistency check, we will now consider the special case of full equilibrium, i.e., of chemical and mechanical equilibrium in addition to thermal equilibrium.

In chemical equilibrium with $\Delta\mu = 0$, the expression (4.8) for the chemical energy change $\Delta\mu(\mathcal{C}_\nu^d)$ during the completion of dicycle $\mathcal{C}_\nu^d$ becomes

$$\Delta\mu(\mathcal{C}_\nu^d) = \sum_{|ij\rangle}^{\nu,d} \Delta\mu_{ij} = 0 \tag{8.5}$$

for any dicycle $\mathcal{C}_\nu^d$ of the network. We can then introduce chemical potentials μ_i for each state i which satisfy

$$\mu_j - \mu_i = \Delta\mu_{ij} \tag{8.6}$$

with $\Delta\mu_{ij} = 0$, $+\mu(X)$, or $-\mu(X)$ as given by relation (4.5). For $\Delta\mu = \mu(\mathrm{ATP}) - \mu(\mathrm{P}) - \mu(\mathrm{ADP}) = 0$, this set of linear equations determines the chemical potentials μ_i up to an additive constant, say μ_o. Using the chemical potentials μ_i, we can now calculate the equilibrium distribution $P_i^{\mathrm{st}} = P_i^{\mathrm{eq}}$ which applies to full equilibrium with $\Delta\mu = 0$ and $F = 0$. In this situation, the energy balance relations (6.10) reduce to the detailed balance conditions $P_i^{\mathrm{eq}}\omega_{ij,0} = P_j^{\mathrm{eq}}\omega_{ji,0}$ as given by (5.5). If we insert this relation into the energy balance relation (6.15) for the transition $|ij\rangle$ together with $\Delta\mu_{ij} = \mu_j - \mu_i$ and $F = 0$, we obtain

$$\frac{P_i^{\mathrm{eq}}}{P_j^{\mathrm{eq}}} = \frac{\exp[-(U_i - \mu_i)/k_B T]}{\exp[-(U_j - \mu_j)/k_B T]}. \tag{8.7}$$

Thus, the equilibrium distribution has the form

$$P_i^{\mathrm{eq}} = \frac{1}{Z}\hat{P}_i^{\mathrm{eq}} \tag{8.8}$$

with the unnormalized probabilities or Gibbs factors

$$\hat{P}_i^{\mathrm{eq}} \equiv \exp[-(U_i - \mu_i)/k_B T] \tag{8.9}$$

and the partition function

$$Z \equiv \sum_i \hat{P}_i^{\mathrm{eq}} = \sum_i \exp[-(U_i - \mu_i)/k_B T]. \tag{8.10}$$

This equilibrium distribution is precisely what we would have obtained from a (restricted) grand canonical ensemble for the motor system which provides a nontrivial consistency check of the theory. The grand-canonical ensemble is restricted since each catalytic domain

can bind at most a single ATP or ADP or the combination $\Theta = \mathrm{ADP/P}$. Note that the distribution $\{P_i^{\mathrm{eq}}\}$ as given by (8.8) is independent of the additive constants U_o and μ_o for the internal energies and chemical potentials. Indeed, if we added such constants in the exponent of the Gibbs factors $\hat{P}_i^{\mathrm{eq}}$, they would be cancelled by the normalization via the partition function Z.

9 Constrained Equilibrium and Nonequilibrium

In this final section, we will reinterpret the local energy balance conditions in terms of constrained equilibria between neighboring motor states. In general, these constrained equilibria can be extended towards trees of the network but not towards all of its cycles. As we try to extend the constrained equilibria to different cycles, we again encounter the nonlocal balance conditions that pinpoint chemical and/or mechanical nonequilibrium.

For each edge $\langle ij \rangle$ of the network representation, the local energy balance relation as given by (6.15) can be rewritten in the form

$$\frac{\omega_{ji}}{\omega_{ij}} = \frac{\exp[-U_i/k_BT]}{\exp[-U_j/k_BT]} e^{(-\Delta\mu_{ij} + \ell_{ij}F)/k_BT}. \tag{9.1}$$

In full equilibrium with $\Delta\mu_{ij} = \mu_j - \mu_i$ and $F = 0$, the motor system is characterized by transition rates $\omega_{ij} = \omega_{ij,0}$ that satisfy the detailed balance condition

$$\frac{\omega_{ji}}{\omega_{ij}} = \frac{\exp[-(U_i - \mu_i)/k_BT]}{\exp[-(U_j - \mu_j)/k_BT]} = \frac{P_i^{\mathrm{eq}}}{P_j^{\mathrm{eq}}} \tag{9.2}$$

as follows from (5.5) and (8.7). It is interesting to note that the relation $\omega_{ji}/\omega_{ij} \sim \exp[(U_j - U_i)/k_BT]$ agrees with both classical transition-state theory and Kramers theory. Indeed, both theories lead to $\omega_{ij} \sim \exp[-(U_{\mathrm{ba},ij} - U_i)/k_BT]$ and $\omega_{ji} \sim \exp[-(U_{\mathrm{ba},ij} - U_j)/k_BT]$ with the energy barrier $U_{\mathrm{ba},ij}$ but this latter barrier drops out from the ratio ω_{ji}/ω_{ij}.

Let us now use the local energy balance as given by (9.1) in order to define two probabilities P_a^{ce} and P_b^{ce} for two neighboring states $i = a$ and $j = b$ in close analogy to the detailed balance relation (9.2). The superscript 'ce' stands for 'constrained equilibrium' as will be explained in the next paragraph. Thus, for a given edge $\langle ab \rangle$, the probabilities P_a^{ce} and P_b^{ce} will be defined via

$$\frac{\omega_{ba}}{\omega_{ab}} = \frac{\exp[-U_a/k_BT]}{\exp[-U_b/k_BT]} e^{(-\Delta\mu_{ab} + \ell_{ab}F)/k_BT} \equiv \frac{P_a^{\mathrm{ce}}}{P_b^{\mathrm{ce}}}. \tag{9.3}$$

We have used the indices a and b rather than the indices i and j in order to emphasize that this definition applies to an arbitrary but fixed edge $\langle ab \rangle$.

For a given edge $\langle ab \rangle$, the two probabilities P_a^{ce} and P_b^{ce} defined by (9.3) have a rather intuitive interpretation in terms of a constrained equilibrium between the neighboring states a and b. Indeed, let us consider the subsystem $\lfloor ab \rfloor$ consisting of the motor states a and b together with the transitions $|ab\rangle$ and $|ba\rangle$. This subsystem is taken to be in thermal equilibrium with the heat reservoir at temperature T. If the chemical energy change $\Delta\mu_{ab}$ during the transition $|ab\rangle$ is zero, see relation (4.5), we do not couple the subsystem $\lfloor ab \rfloor$ to any particle reservoir. On the other hand, if $\Delta\mu_{ab} = \pm\mu(X)$, we couple $\lfloor ab \rfloor$ only to the particle reservoir for the chemical species X. Likewise, we couple the subsystem to the work

reservoir only if the mechanical displacement $\ell_{ab} \neq 0$. This constrained equilibrium of the subsystem $\lfloor ab \rfloor$ is governed by the probabilities $P_a^{\rm ce}$ and $P_b^{\rm ce}$ which satisfy relation (9.3). Thus, the latter relation corresponds to the detailed balance condition for the constrained equilibrium of subsystem $\lfloor ab \rfloor$.

The concept of a constrained equilibrium between two neighboring states has been previously discussed by T.L. Hill in [19, 43] (who called it a 'hypothetical equilibrium'). His relations differ from ours in two ways. First, his constrained equilibrium relations are restricted to $F = 0$ since he did not include a work reservoir. Second, in our notation, his relations have the form

$$\frac{\omega_{ba}}{\omega_{ab}} = \frac{\exp[-H_a/k_BT]}{\exp[-H_b/k_BT]} e^{-\Delta\mu_{ab}/k_BT} \tag{9.4}$$

where H_a and H_b are the Helmholtz free energies of the states a and b as defined in (4.2). A similar relation has been proposed more recently in [58] where the Helmholtz free energy was replaced by the grand-canonical potential. In contrast, our theory leads to constrained equilibrium relations which depend on the internal energies U_a and U_b as in (9.3) rather than on the Helmholtz or grand-canonical free energies. Our result (9.3) for the constrained equilibria is equivalent to energy conservation during the transition $|ij\rangle$ together with the expression $Q_{ij} = T\Delta S_{ij} = k_BT \ln(\omega_{ij}/\omega_{ji})$ for the heat exchange Q_{ij} during the transition $|ij\rangle$. The consistency of our scheme is confirmed by our explicit expressions for the internal energies as given by (8.2–8.4).

There is one important difference between the relation (9.2) for full equilibrium and the relation (9.3) for constrained equilibrium. For full equilibrium, the probability ratio $P_i^{\rm eq}/P_j^{\rm eq}$ depends only on the internal energy U_i and the chemical potential μ_i, i.e., on quantities that characterize the individual motor states i. In contrast, the probability ratio $P_a^{\rm ce}/P_b^{\rm ce}$ for the constrained equilibrium of subsystem $\lfloor ab \rfloor$ also involves the chemical energy change $\Delta\mu_{ab}$ and the mechanical work $W_{{\rm me},ab} = \ell_{ab}F$, two quantities that characterize the transition $|ab\rangle$ rather than the individual states a and b. As long as we consider a single subsystem $\lfloor ab \rfloor$, this difference is not crucial since we can then introduce chemical potentials μ_a and μ_b and load force potentials V_a and V_b via

$$\Delta\mu_{ab} \equiv \mu_b - \mu_a \quad \text{and} \quad \ell_{ab}F \equiv V_b - V_a. \tag{9.5}$$

In fact, it is possible to extend this latter definition to all edges of a spanning tree of the network graph $\mathbb{G}$. Such a tree consists of all $N_{\rm s}$ motor states (or vertices) together with $N_{\rm s} - 1$ edges, which form a subgraph without any cycle, see, e.g., [59].

However, as soon as we add another edge to such a spanning tree and close one cycle of the network, say $\mathcal{C}_n$, the chemical potentials μ_a can only be defined on the whole subgraph if

$$\Delta\mu(\mathcal{C}_n^d) = \sum_{|ab\rangle}^{n,+} \Delta\mu_{ab} = 0, \tag{9.6}$$

i.e., if the cycle $\mathcal{C}_n$ is in chemical equilibrium. Likewise, the load force potentials V_a can only be defined for the subgraph including $\mathcal{C}_n$ if

$$W_{\rm me}(\mathcal{C}_n^d) = \sum_{|ab\rangle}^{n,+} \ell_{ab}F = 0, \tag{9.7}$$

i.e., if the cycle $\mathcal{C}_n$ is in mechanical equilibrium.

The conditions (9.6) and (9.7) for chemical and mechanical equilibrium of single cycles were previously introduced in Sect. 4.3 and are directly related to the cycle classification in Sect. 3.3. A thermal slip cycle $\mathcal{C}_n$ is both in chemical and in mechanical equilibrium. A mechanical slip cycle $\mathcal{C}_n$ is in chemical equilibrium but in mechanical nonequilibrium, i.e., $W_{\rm me}(\mathcal{C}_n^d) \neq 0$. A dissipative slip cycle $\mathcal{C}_n$ is in mechanical equilibrium but in chemical nonequilibrium, i.e., $\Delta\mu(\mathcal{C}_n^d) \neq 0$. Finally, a chemomechanical cycle is both in mechanical and in chemical nonequilibrium.

In order to discuss the global situation corresponding to the whole network, let us recall some additional terminology as used in graph theory, see, e.g., [59]. We decompose the network graph $\mathbb{G}$ into a certain spanning tree $\mathcal{T}$ and its cotree $\mathcal{T}^{\rm c}$, which consists of all edges of $\mathbb{G}$ not contained in $\mathcal{T}$. If the network has $N_{\rm e}$ edges, the cotree $\mathcal{T}^{\rm c}$ has $N_{\rm e}^{\rm c} = N_{\rm e} - N_{\rm s} + 1$ edges denoted by $\epsilon_n^{\rm c}$ with $n = 1, 2, \ldots, N_{\rm e}^{\rm c}$. When we add the edge $\epsilon_n^{\rm c}$ to the spanning tree $\mathcal{T}$, we obtain a subgraph of $\mathbb{G}$ which contains the cycle $\mathcal{C}_n$ but no other cycle. The set of cycles $\mathcal{C}_n$ with $n = 1, 2, \ldots, N_{\rm e}^{\rm c}$ forms a so-called fundamental set of cycles; all other cycles of the network can be obtained by cycle addition which corresponds to the operation of symmetric difference applied to the edge sets of these cycles. In general, the symmetric difference of two sets A and B is defined by $A + B \equiv (A \cup B) \setminus (A \cap B)$.

If the constrained chemical equilibrium (9.6) holds for all cycles $\mathcal{C}_n$ of a certain fundamental set of cycles, it holds for all cycles of the network which implies that the motor is in chemical equilibrium and $\Delta\mu = 0$. Likewise, if the constrained mechanical equilibrium (9.7) holds for all cycles $\mathcal{C}_n$ of the fundamental set, it holds for all cycles of the network which implies that the motor is in mechanical equilibrium and $F = 0$. Finally, if constrained chemical as well as mechanical equilibrium holds for all cycles $\mathcal{C}_n$ of the fundamental set, the motor is in full equilibrium and we can extend the constrained equilibrium condition (9.3) for the subsystem $\lfloor ab \rfloor$ to the whole network with equilibrium probabilities $P_a^{\rm ce} = P_a^{\rm eq}$ and $P_b^{\rm ce} = P_b^{\rm eq}$ for all edges $\langle ab \rangle$ and dicycle ratios $\Xi(\mathcal{C}_\nu^d) = 1$ for all dicycles $\mathcal{C}_\nu^d$ as in (5.7).

On the other hand, as soon as we encounter any cycle $\mathcal{C}_n$ for which the constrained chemical equilibrium (9.6) and/or the constrained mechanical equilibrium (9.7) does not hold, we can no longer extend the definitions (9.5) for the chemical potentials μ_a and/or the load force potentials V_a to the whole subgraph. This break-down of constrained equilibrium, which implies dicycle ratios $\Xi(\mathcal{C}_n^d) \neq 1$, is precisely revealed by the nonlocal balance conditions as given by (6.9) and (6.10).

10 Summary and Outlook

In summary, our theoretical framework has three basic ingredients as discussed in Sects. 2–4: (i) The thermodynamic description of the motor and its reservoirs; (ii) Network representations of the motor based on the motor states i and the transitions $|ij\rangle$ from state i to state j; and (iii) The energy balance relations (4.4) and (4.10) for single transitions and dicycles of the network, respectively. The basic ingredients (i)–(iii) are rather general and do not involve any assumptions about the motor dynamics. In order to proceed any further, one has to consider a specific dynamics of the motor molecule.

In Sect. 5, we considered the presumably simplest motor dynamics in terms of a continuous-time Markov process on the network of motor states. This dynamics allows us to calculate various steady state properties such as the entropy produced by the motor during a completed dicycle and during a single transition as given by (6.8) and (6.13), respectively. When we identify the entropy produced during a completed dicycle with the heat exchange during this dicycle, we obtain the energy balance relation (6.10) between the dicycle ratio

$\Xi(\mathcal{C}_\nu^d)$ of the transition rates and the thermodynamic control parameters. When we identify the transition entropy with the heat exchange during the transition $|ij\rangle$, we obtain the local energy balance relation (6.15) between the internal energy difference $U_j - U_i$, the chemical energy change $\Delta\mu_{ij}$, the mechanical work $\ell_{ij}F$, and the transition rate ratio ω_{ij}/ω_{ji}.

In Sect. 7, we viewed the energy balance relations (6.10) and (6.15) as balance *conditions* that have to be satisfied by the transition rates ω_{ij} in order to obtain a dynamic model that is consistent with thermodynamics. These conditions have several important consequences. First, the nonlocal balance conditions (7.9) and (7.10) relate (i) the zero-force transition rates $\omega_{ij,0}$ of a dicycle to the overall energy change $\Delta\mu$ per ATP hydrolyis and (ii) the load-dependent factors Φ_{ij} to the load force F. Thus, using these balance conditions, one can estimate unknown transition rates of the motor in terms of known ones as we have previously shown for kinesin [17]. Second, the local balance conditions (7.12) and the obvious requirement that the internal energies U_i must be independent of the concentrations or activities $[X]$ and of the load force F lead to rather strong constraints on the dependence of the transition rates ω_{ij} on these thermodynamic parameters: (i) to the parametrization (7.17) for the zero-force transition rates $\omega_{ij,0}$, (ii) to the condition $\Phi_{ij}/\Phi_{ji} = \exp[-\ell_{ij}F/k_BT]$ for the load-dependent factors $\Phi_{ij} = \Phi_{ij}(F)$ as in (7.13), and (iii) to the simple relation $\zeta_{ij} = \zeta_{ji}$ for the additional force-dependent factors $\zeta_{ij}(F, \mathbf{F}_\perp)$ as in (7.14). Third, the local balance condition (7.12) allows us to determine the internal energies U_i of the motor, see (8.2–8.4), and the equilibrium distribution as given by (8.8).

Finally, we have reinterpreted the local balance conditions in terms of constrained equilibria between neighboring motor states, see relation (9.3). When we combine these constrained equilibria and try to extend them to the whole network, we detect chemical and/or mechanical nonequilibrium as soon as we encounter cycles $\mathcal{C}_n$ with $\Delta\mu(\mathcal{C}_n^d) \neq 0$ and/or $W_{\rm me}(\mathcal{C}_n^d) \neq 0$, compare the relations (9.6) and (9.7). These relations are equivalent to the nonlocal balance conditions as given by (7.9) and (7.10).

The theoretical framework presented here is very economical and incorporates the "principle of Occam's razor". It involves only two types of parameters: (i) thermodynamic parameters that characterize the different reservoirs and (ii) the transition rates ω_{ij} that govern the motor dynamics. Both types of parameters can be measured, at least in principle, and all other quantities that appear in our theory can be expressed in terms of these parameters. In particular, these two types of parameters also determine the landscape of internal energies U_i: Indeed, inspection of (8.2–8.4) shows that the internal energies U_i can be expressed in terms of the rate constants κ_{ij} and the activity scales $[X]^*$. Thus, the energy landscape $\{U_i\}$ must not be considered as an independent set of parameters. The latter remark also applies to ratchet models with spatially localized transitions since these latter models are equivalent to the network models considered here as shown in [28, 29].

As mentioned in the introduction, our theoretical approach has already been successfully applied to the molecular motor kinesin [16–18]. Most of the experimental results on kinesin can be understood in terms of the 6-state network as in Fig. 4(c) which we display in a slightly different way in Fig. 5(a). In order to understand the strong decrease of the motor velocity with increasing ADP concentration [15], we found it necessary to enlarge the state space and to include another motor state in which both motor domains are occupied by ADP; the resulting 7-state model is shown in Fig. 5(b). Both the 6-state and the 7-state model have the simplifying feature that they involve only a single mechanical step represented by the broken edge $\langle 25\rangle$. Using these network representations, one can calculate all motor properties that have been observed in single molecule experiments [17] and determine additional properties such as ATP hydrolysis rate and motor efficiency [60] as well as the sojourn (or waiting) time distribution for the effective stochastic process that consists of the mechanical steps alone [61].

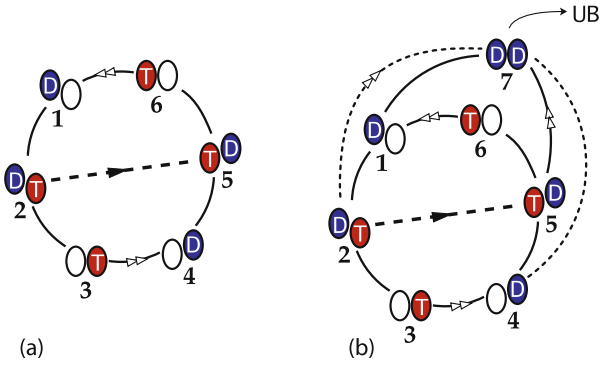

Fig. 5 Network models for kinesin: (**a**) 6-state network as in Fig. 4(c) with two chemomechanical cycles, the forward cycle $\mathcal{F} = \langle 12561 \rangle$ and the backward cycle $\mathcal{B} = \langle 23452 \rangle$. The direction of the forward mechanical step is now indicated by the *black arrow* and the direction of the ATP hydrolysis by *white double-arrows*; and (**b**) 7-state network with two additional chemomechanical cycles, the additional forward cycle $\mathcal{F}_{\mathrm{DD}} = \langle 12712 \rangle$ and the additional backward cycle $\mathcal{B}_{\mathrm{DD}} = \langle 27452 \rangle$. In the limit of small ADP concentration, the observed dependence of the motor properties on the load force arises from the competition of the forward cycle $\mathcal{F}$ and the backward cycle $\mathcal{B}$. In the limit of small load force, on the other hand, the available experimental data on the ADP dependence of the motor velocity can be understood from the concerted action of the two forward cycles $\mathcal{F}$ and $\mathcal{F}_{\mathrm{DD}}$ [17]. The unbinding (UB) of the motor from the filament is most likely to occur from the weakly bound state (D, D)

It would also be interesting to abandon the assumption of a continuous-time Markov process, which is governed by the exponential distribution $P(\tau_i) = (1/\langle \tau_i \rangle) \exp[-\tau_i/\langle \tau_i \rangle]$ for the sojourn (or dwell) time τ_i of motor state i as in (5.1), and to consider more general, nonexponential distributions $P(\tau_i) = P^{\mathrm{ne}}(\tau_i)$. Indeed, for real motor molecules, the distributions $P(\tau_i)$ must vanish for small τ_i in contrast to the exponential distribution of the Markov process as given by (5.1). In addition, since each motor state i contains many substates (i, k), see Sect. 4.1, the sojourn time distribution $P(\tau_i)$ might be governed by more than one time scale. The theoretical framework described here strongly suggests that the corresponding non-Markov process will again be characterized by local and nonlocal balance relations as in (6.10) and (6.15) provided the transition rates ω_{ij} are replaced by $\pi_{ij}/\langle \tau_i \rangle$ as in (5.3) and the average values $\langle \tau_i \rangle$ of the sojourn times are calculated using the distributions $P^{\mathrm{ne}}(\tau_i)$.

Other two-headed motors could be modelled in a rather similar fashion as kinesin. Myosin V, for example, has two catalytic domains as well and, thus, would be described by the same network of chemical transitions as in Fig. 4(a). Dynein, on the other hand, has several ATP binding domains per head and, thus, may have $M > 2$ catalytically active domains. In the latter case, one would have to consider a more complex state space with 3^M states. Likewise, one might apply our approach to motors that couple ATP hydrolysis with work against a concentration gradient. A prominent example is provided by $F_o F_1$-ATPase which has been studied in some detail using the framework of ratchet or Fokker-Planck models [62]. Finally, it would be desirable to extend the theoretical framework presented here to the growth of cytoskeletal filaments, for which the number M of catalytic domains is not fixed but grows with the filament length.

Acknowledgements We thank Angelo Valleriani for stimulating discussions as well as Frank Jülicher and Udo Seifert for useful correspondence. S.L. was supported by the EC sixth Framework Program (STREP Contract No. NMP4-CT-2004-516989).

Appendix: Single Catalytic Motor Domain

In this appendix, we will discuss the simple example of a single catalytic motor domain as shown in Fig. 3. The 4-state network in Fig. 3(a) was previously used by T.L. Hill [19] to model a generic ATPase that does not perform any mechanical work. We will first review the energy balance relation for the 4-state network and then show that the reduction of the 4-state to the 3-state network does not change the energy transduction of the ATPase cycle.

11.1 Energy Transduction in 4-State Network

For the 4-state network in Fig. 3(a), the dissipative slip dicycle $\mathcal{D}_{4s}^{+} = |\mathrm{ET\Theta DE}\rangle$ is governed by the energy balance relation

$$Q(\mathcal{D}_{4s}^{+}) = T\,\Delta S(\mathcal{D}_{4s}^{+}) = k_B T \ln\left(\frac{\omega_{\mathrm{ET}}\omega_{\mathrm{T\Theta}}\omega_{\mathrm{\Theta D}}\omega_{\mathrm{DE}}}{\omega_{\mathrm{TE}}\omega_{\mathrm{\Theta T}}\omega_{\mathrm{D\Theta}}\omega_{\mathrm{ED}}}\right) = \Delta\mu. \tag{11.1}$$

This relation is intuitively obvious. The catalytic domain obtains the chemical energy $\Delta\mu$ by hydrolyzing one ATP molecule during one completed dicycle $\mathcal{D}_{4s}^{+}$, and this chemical energy is completely converted into heat in the absence of any mechanical work.

The last equality in the energy balance relation (11.1) has been previously derived by T.L. Hill in [19] using the following line of reasoning. First, he assumed that all transitions $|ij\rangle$, which involve the binding of one of the chemical species X = ATP, ADP or P, have transition rates ω_{ij} that are proportional to the activity or molar concentration $[X]$ whereas all other rates ω_{ij} are independent of $[X]$. Second, using this parametrization of the transition rates in the detailed balance condition $k_B T \ln[\Xi(\mathcal{D}_{4s}^{+})] = 1$ as in (5.7), Hill obtained

$$\frac{\kappa_{\mathrm{ET}}\kappa_{\mathrm{T\Theta}}\kappa_{\mathrm{\Theta D}}\kappa_{\mathrm{DE}}}{\kappa_{\mathrm{TE}}\kappa_{\mathrm{\Theta T}}\kappa_{\mathrm{D\Theta}}\kappa_{\mathrm{ET}}} = \frac{[\mathrm{ADP}][\mathrm{P}]}{[\mathrm{ATP}]}\bigg|^{\mathrm{eq}} = K^{\mathrm{eq}} \tag{11.2}$$

where the last equality follows from the relation (2.6) for the equilibrium constant K^{eq}. Finally, combining this relation between the rate constants and the equilibrium constant with the thermodynamic relation (2.5), Hill concludes that the relation (11.1) holds for any state of the system. This line of reasoning was extended to general biochemical networks in [63, 64]. Obviously, our derivation of (11.1) is different and relies on the energy balance during the completion of dicycle $\mathcal{D}_{4s}^{+}$ together with the identity $Q(\mathcal{D}_{4s}^{+}) = T\,\Delta S(\mathcal{D}_{4s}^{+})$.

11.2 Reduction to 3-State Network

Now, let us assume that we have determined the transition rates ω_{ij} of the 4-state network in Fig. 3(a) in such a way that they satisfy the energy (or steady state) balance condition (11.1). We now reduce this 4-state network and eliminate the state Θ which leads to the 3-state network in Fig. 3(b). How do we have to choose the transition rates of the reduced 3-state network in order to preserve the thermodynamic consistency of the 4-state network?

For the 3-state network in Fig. 3(b), the dissipative slip dicycle $\mathcal{D}_{3s}^{+} \equiv |\mathrm{ETDE}\rangle$ is governed by the energy balance relation

$$Q(\mathcal{D}_{3s}^{+}) = T\,\Delta S(\mathcal{D}_{3s}^{+}) = k_B T \ln\left(\frac{\omega_{\mathrm{ET}}\omega_{\mathrm{TD}}\omega_{\mathrm{DE}}}{\omega_{\mathrm{TE}}\omega_{\mathrm{DT}}\omega_{\mathrm{ED}}}\right) = \Delta\mu. \tag{11.3}$$

We now require that both networks describe the same energy transduction for the same value of $\Delta\mu$. Comparison of the two steady state balance conditions (11.1) and (11.3) then implies the constraint

$$\frac{\omega_{\mathrm{TD}}}{\omega_{\mathrm{DT}}} = \frac{\omega_{\mathrm{T}\Theta}\omega_{\Theta\mathrm{D}}}{\omega_{\Theta\mathrm{T}}\omega_{\mathrm{D}\Theta}} \tag{11.4}$$

for the transition rates ω_{TD} and ω_{DT} of the 3-state network in terms of the transition rates $\omega_{\mathrm{T}\Theta}$, $\omega_{\Theta\mathrm{T}}$, $\omega_{\Theta\mathrm{D}}$ and $\omega_{\mathrm{D}\Theta}$ of the 4-state network.

The relation (11.4) may also be expressed in terms of the transition entropies $\Delta S_{ij} = k_B \ln(\omega_{ij}/\omega_{ji})$ or the corresponding heat exchanges $Q_{ij} = T\Delta S_{ij}$ which leads to

$$\Delta S_{\mathrm{TD}} = \Delta S_{\mathrm{T}\Theta} + \Delta S_{\Theta\mathrm{D}} \quad \text{or} \quad Q_{\mathrm{TD}} = Q_{\mathrm{T}\Theta} + Q_{\Theta\mathrm{D}}. \tag{11.5}$$

This gives a direct physical interpretation of the constraint (11.4): When we combine the hydrolysis transition $|\mathrm{T}\Theta\rangle$ with the P release transition $|\Theta\mathrm{D}\rangle$ into the new, effective transition $|\mathrm{TD}\rangle$, we want the heat Q_{TD} exchanged during the transition $|\mathrm{TD}\rangle$ to be equal to the sum of the two heats exchanged during the transitions $|\mathrm{T}\Theta\rangle$ and $|\Theta\mathrm{D}\rangle$.

Furthermore, using the local balance conditions (6.15), we also find that the constraint (11.4) implies the relation

$$\Delta U_{\mathrm{TD}} = -\mu(\mathrm{P}) - k_B T \ln\left(\frac{\omega_{\mathrm{TD}}}{\omega_{\mathrm{DT}}}\right) = \Delta U_{\mathrm{T}\Theta} + \Delta U_{\Theta\mathrm{D}} \tag{11.6}$$

between the internal energy differences $\Delta U_{\mathrm{T}\Theta}$ and $\Delta U_{\Theta\mathrm{D}}$ in the 4-state model and the internal energy difference ΔU_{TD} in the 3-state model. Thus, the constraint (11.4) ensures that the energy landscape of the remaining states E, T, and D is not affected by the elimination of the state Θ.

Glossary of Mathematical Symbols

ADP	adenosine diphosphate.
ATP	adenosine triphosphate.
$\mathcal{B}$	chemomechanical backward cycle in Figs. 4 and 5.
$\mathcal{C}_\nu$	cycle of network graph labeled by index ν.
$\mathcal{C}_\nu^d$	directed cycle or dicycle of network graph with direction d.
d	direction of dicycle with $d = \pm$.
$\mathcal{D}$	dissipative slip cycle.
$E_{i,k}$	energies of substates (i,k) of motor state i.
$\mathbb{G}$	graph of network; the vertices of $\mathbb{G}$ are the motor states i, the edges $\langle ij\rangle$ of $\mathbb{G}$ represent the two transitions $\|ij\rangle$ and $\|ji\rangle$.
ΔJ_{ij}	local excess flux of transition $\|ij\rangle$ with $\Delta J_{ij} = J_{ij} - J_{ji}$.
$\Delta\mu$	chemical energy change per ATP hydrolysis as defined in (2.4).
$\Delta\mu_{ij}$	chemical energy change during transition $\|ij\rangle$.
$\Delta\mu(\mathcal{C}_\nu^d)$	chemical energy change during dicycle $\mathcal{C}_\nu^d$.
ΔS_{ij}	entropy produced during transition $\|ij\rangle$.
$\Delta S(\mathcal{C}_\nu^d)$	entropy produced during the completion of dicycle $\mathcal{C}_\nu^d$.
ΔU_{ij}	internal energy change during transition $\|ij\rangle$ with $\Delta U_{ij} = U_j - U_i$.
F	load force acting on the motor parallel to the filament; $F > 0$ for resisting load.
$\vec{F}_{\mathrm{ex}}$	3-dimensional vector of externally applied force with $\vec{F}_{\mathrm{ex}} = (F, \mathbf{F}_\perp)$ as in (2.2).

$\mathbf{F}_\perp$	2-dimensional force acting on the motor perpendicular to the filament.
$\mathcal{F}$	chemomechanical forward cycle in Figs. 4 and 5.
H_i	Helmholtz free energy of motor state i.
i and j	discrete motor states.
$\|ij\rangle$	transition or directed edge (di-edge) from motor state i to state j.
$\langle ij\rangle$	edge between states i and j.
(i,k)	substates of motor state i.
J_{ij}	probability flux from motor state i to state j with $J_{ij} = P_i\omega_{ij}$.
κ_{ij}	rate constant for transition from state i to state j.
k_B	Boltzmann constant.
K^{eq}	equilibrium constant for ATP hydrolysis as defined in (2.6).
ℓ	mechanical displacement of motor.
ℓ_{ij}	mechanical motor displacement during transition $\|ij\rangle$.
$\ell(\mathcal{C}_\nu^d)$	mechanical motor displacement during completion of dicycle $\mathcal{C}_\nu^d$.
M	number of catalytic domains.
μ	chemical potential.
$\mu(X)$	chemical potential for chemical species X as given by (2.5).
μ_i	chemical potential for motor state i in chemical equilibrium.
ν	label for all cycles in the network.
ω_{ij}	transition rate for transition from motor state i to state j.
$\omega_{ij,0}$	transition rates for zero external force as defined in (7.2).
$\Omega_{ij}^{\mathrm{st}}$	frequency of transition $\|ij\rangle$ in the steady state.
$\Omega^{\mathrm{st}}(\mathcal{C}_\nu^d)$	frequency of completion of dicycle $\mathcal{C}_\nu^d$ in the steady state.
P	inorganic phosphate.
P_i	probability to find the motor in state i.
P_i^{st}	probability for motor state i if the system is in its steady state.
P_i^{eq}	probability for motor state i if the system is in its equilibrium state.
π_{ij}	transition probability for transition from state i to state j.
Φ_{ij}	load-dependent factor of transition rate ω_{ij} as defined in (7.3).
Q_{ij}	heat released by the motor during transition $\|ij\rangle$.
$Q(\mathcal{C}_\nu^d)$	heat released by the motor during completion of dicycle $\mathcal{C}_\nu^d$.
σ_{fl}	entropy flux of motor system as defined in (6.4).
σ_{pr}	entropy production rate of motor system as defined in (6.3).
$\sigma_{\mathrm{pr}}^{\mathrm{st}}$	entropy production rate in the steady state of the motor system.
t	time.
T	temperature.
$\mathcal{T}$	spanning tree of network graph.
$\mathcal{T}^c$	cotree of spanning tree $\mathcal{T}$.
τ_i	sojourn or dwell time in motor state i.
U_i	internal energy of motor state i.
V_a	load force potential for motor state a.
W_{me}	mechanical work performed by the motor.
$W_{\mathrm{me},ij}$	mechanical work performed by the motor during transition $\|ij\rangle$.
X	chemical species ATP, ADP or P.
$[X]$	activity or molar concentration of chemical species X.
$[X]^*$	activity scale for chemical species X as given by (2.3).
ζ_{ij}	force-dependent factor of the transition rate ω_{ij} as defined in (7.4).
$\Xi(\mathcal{C}_\nu^d)$	dicycle ratio for dicycle $\mathcal{C}_\nu^d$ as defined in (5.6).
$\Xi_0(\mathcal{C}_\nu^d)$	zero-force dicycle ratio for dicycle $\mathcal{C}_\nu^d$ as defined in (7.6).

$\Xi_F(\mathcal{C}_\nu^d)$ load-dependent factor of dicycle ratio $\Xi(\mathcal{C}_\nu^d)$ as defined in (7.7).
$\Xi_\perp(\mathcal{C}_\nu^d)$ $\mathbf{F}_\perp$-dependent factor of dicycle ratio $\Xi(\mathcal{C}_\nu^d)$ as defined in (7.8).
Z grand-canonical partition function of motor states, see (8.10).
Z_i canonical partition function of substates for motor state i, see (4.1).

References

1. Howard, J.: Mechanics of Motor Proteins and the Cytoskeleton, 1 edn. Sinauer, New York (2001)
2. Schliwa, M., Woehlke, G.: Molecular motors. Nature **422**, 759–765 (2003)
3. Vale, R.D.: The molecular motor toolbox for intracellular transport. Cell **112**, 467–480 (2003)
4. Mallik, R., Gross, S.P.: Molecular motors: Strategies to get along. Curr. Biol. **14**, R971–R982 (2004)
5. Svoboda, K., Schmidt, C.F., Schnapp, B.J., Block, S.M.: Direct observation of kinesin stepping by optical trapping interferometry. Nature **365**, 721–727 (1993)
6. Yildiz, A., Tomishige, M., Vale, R.D., Selvin, P.R.: Kinesin walks hand-over-hand. Science **303**, 676–678 (2004)
7. Carter, N.J., Cross, R.A.: Mechanics of the kinesin step. Nature **435**, 308–312 (2005)
8. Schnitzer, M.J., Block, S.M.: Kinesin hydrolyses one ATP per 8-nm step. Nature **388**, 386–390 (1997)
9. Hackney, D.D.: The tethered motor domain of a kinesin-microtubule complex catalyzes reversible synthesis of bound ATP. Proc. Natl. Acad. Sci. **102**, 18338–18343 (2005)
10. Gilbert, S.P., Moyer, M.L., Johnson, K.A.: Alternating site mechanism of the kinesin ATPase. Biochemistry **37**, 792–799 (1998)
11. Romberg, L., Vale, R.D.: Chemomechanical cycle of kinesin differs from that of myosin. Nature **361**, 168–170 (1993)
12. Guydosh, N.R., Block, S.M.: Backsteps induced by nucleotide analogs suggest the front head of kinesin is gated by strain. Proc. Natl. Acad. Sci. **103**, 8054–8059 (2006)
13. Visscher, K., Schnitzer, M.J., Block, S.M.: Single kinesin molecules studied with a molecular force clamp. Nature **400**, 184–189 (1999)
14. Schnitzer, M.J., Visscher, K., Block, S.M.: Force production by single kinesin motors. Nature Cell Biol. **2**, 718–723 (2000)
15. Schief, W.R., Clark, R.H., Crevenna, A.H., Howard, J.: Inhibition of kinesin motility by ADP and phosphate supports a hand-over-hand mechanism. Proc. Natl. Acad. Sci. **101**, 1183–1188 (2004)
16. Liepelt, S., Lipowsky, R.: Steady-state balance conditions for molecular motor cycles and stochastic nonequilibrium processes. Europhys. Lett. **77**, 50002 (2007)
17. Liepelt, S., Lipowsky, R.: Kinesin's network of chemomechanical motor cycles. Phys. Rev. Lett. **98**, 258102 (2007)
18. Lipowsky, R., Chai, Y., Klumpp, S., Liepelt, S., Müller, M.J.I.: Molecular motor traffic: From biological nanomachines to macroscopic transport. Physica A **372**, 34–51 (2006)
19. Hill, T.L.: Free Energy Transduction and Biochemical Cycle Kinetics, 1 edn. Springer, New York (1989)
20. Peskin, C.S., Oster, G.: Coordinated hydrolysis explains the mechanical behavior of kinesin. Biophys. J. **68**, 202S (1995)
21. Jülicher, F., Ajdari, A., Prost, J.: Modeling molecular motors. Rev. Mod. Phys. **69**, 1269–1281 (1997)
22. Parmeggiani, A., Jülicher, F., Ajdari, A., Prost, J.: Energy transduction of isothermal ratchets: Generic aspects and specific examples close to and far from equilibrium. Phys. Rev. E **60**, 2127–2140 (1999)
23. Fisher, M.E., Kolomeisky, A.: The force exerted by a molecular motor. Proc. Natl. Acad. Sci. **96**, 6597–6602 (1999)
24. Lipowsky, R., Harms, T.: Molecular motors and nonuniform ratchets. Eur. Biophys. J. **29**, 542–548 (2000)
25. Lipowsky, R.: Universal aspects of the chemo-mechanical coupling for molecular motors. Phys. Rev. Lett. **85**, 4401–4404 (2000)
26. Fisher, M.E., Kolomeisky, A.: Simple mechanochemistry describes the dynamics of kinesin molecules. Proc. Natl. Acad. Sci. **98**, 7748–7753 (2001)
27. Qian, H.: Nonequilibrium steady state circulation and heat dissipation functional. Phys. Rev. E **64**, 022101 (2001)
28. Lipowsky, R., Jaster, N.: Molecular motor cycles: From ratchets to networks. J. Stat. Phys. **110**, 1141–1167 (2003)
29. Lipowsky, R., Klumpp, S.: Life is motion—multiscale motility of molecular motors. Physica A **352**, 53–112 (2005)
30. Fisher, M.E., Kim, Y.C.: Kinesin crouches to sprint but resists pushing. Proc. Natl. Acad. Sci. **102**, 16209–16214 (2005)

31. Seifert, U.: Fluctuation theorem for a single enzym or molecular motor. Europhys. Lett. **70**, 36–41 (2005)
32. Qian, H.: Open-System nonequilibrium steady state: Statistical thermodynamics, fluctuations, and chemical oscillations. J. Phys. Chem. B **110**, 15063–15074 (2006)
33. Polanyi, M., Wigner, E.: Über die Interferenz von Eigenschwingungen als Ursache von Energieschwankungen und chemischen Umsetzungen. Z. Phys. Chem. (Leipzig) A **139**, 439–452 (1928)
34. Eyring, H.: The activated complex in chemical reactions. J. Chem. Phys. **3**, 107–115 (1935)
35. Kramers, H.A.: Brownian motion in a field of force and the diffusion model of chemical reactions. Physica (Utrecht) **7**, 284–304 (1940)
36. Hänggi, P., Talkner, P., Borkovec, M.: Reaction-rate theory: Fifty years after Kramers. Rev. Mod. Phys. **62**, 251–341 (1990)
37. van Kampen, N.G.: Stochastic Processes in Physics and Chemistry. Elsevier, Amsterdam (1992)
38. Hill, T.L.: Theoretical formulation for the sliding filament model of contraction of striated muscle: Part I. Prog. Biophys. Mol. Biol. **28**, 267–340 (1974)
39. Jülicher, F.: Force and motion generation of molecular motors: A generic description. In: Müller, S., Parisi, J., Zimmermann, W. (eds.) Transport and Structure, p. 46. Springer, Berlin (1999)
40. Seifert, U.: Entropy production along a stochastic trajectory and an integral fluctuation theorem. Phys. Rev. Lett. **95**, 040602/1–040602/4 (2005)
41. Schmiedl, T., Speck, T., Seifert, U.: Entropy production for mechanically or chemically driven biomolecules. J. Stat. Phys. **128**, 77–93 (2007)
42. Alberty, R.A.: Thermodynamics of the hydrolysis of ATP as a function of temperature, pH, pMg, and ionic strength. J. Phys. Chem. B **107**, 12324–12330 (2003)
43. Hill, T.L., Simmons, R.M.: Free energy levels and entropy production associated with biochemical kinetic diagrams. Proc. Natl. Acad. Sci. **73**, 95–99 (1976)
44. Norris, J.R.: Markov Chains. Cambridge University Press, Cambridge (1997)
45. Kirchhoff, G.: Über die Auflösung der Gleichungen, auf welche man bei der Untersuchung der linearen Verteilung galvanischer Ströme geführt wird. Ann. Phys. Chem. **72**, 497–508 (1847)
46. Tutte, W.T.: Graph Theory. Cambridge University Press, Cambridge (2001)
47. Hill, T.L.: Studies in irreversible thermodynamics, IV, diagrammatic representation of steady state fluxes for unimolecular systems. J. Theor. Biol. **10**, 442–459 (1966)
48. Schnakenberg, J.: Network theory of microscopic and macroscopic behavior of master equation systems. Rev. Mod. Phys. **48**, 571–585 (1976)
49. Hill, T.L., Chen, Y.-D.: Stochastics of cycle completions (fluxes) in biochemical kinetic diagrams. Proc. Natl. Acad. Sci. **72**, 1291–1295 (1975)
50. Kohler, H.-H., Vollmerhaus, E.: The frequency of cyclic processes in biological multistate systems. J. Math. Biol. **9**, 275–290 (1980)
51. Luo, J.L., van den Broeck, C., Nicolis, G.: Stability criteria and fluctuations around non-equilibrium states. Z. Physik B **56**, 165–170 (1984)
52. Lebowitz, J.L., Spohn, H.: A Gallavotti–Cohen-type symmetry in the large deviation functional for stochastic dynamics. J. Stat. Phys. **95**, 333–365 (1999)
53. Maes, C., van Wieren, M.H.: A Markov model for kinesin. J. Stat. Phys. **112**, 329–355 (2003)
54. De Groot, S.R., Mazur, P.: Grundlagen der Thermodynamik irreversibler Prozesse. Hochschultaschenbücher-Verlag, Bibliographisches Institut, Mannheim (1969)
55. Evans, D.J., Cohen, E.G.D., Morris, G.P.: Probability of second law violations in shearing steady states. Phys. Rev. Lett. **71**, 2401–2404 (1993)
56. Crooks, G.E.: Entropy production fluctuation theorem and the nonequilibrium work relation for free energy differences. Phys. Rev. E **60**, 2721–2726 (1999)
57. Jarzynski, C.: Hamiltonian derivation of a detailed fluctuation theorem. J. Stat. Phys. **98**, 77–102 (2000)
58. Andrieux, D., Gaspard, P.: Fluctuation theorems and the nonequilibrium thermodynamics of molecular motors. Phys. Rev. E **74**, 011906 (2006)
59. Wallis, W.D.: A Beginners Guide to Graph Theory. Birkhäuser, Boston (2000)
60. Liepelt, S., Lipowsky, R.: ATP hydrolysis rate and efficiency of the molecular motor kinesin. (In preparation)
61. Valleriani, A., Liepelt, S., Lipowsky, R.: Sojourn time distribution for kinesin's mechanical steps. (In preparation)
62. Xing, J., Liao, J.-C., Oster, G.: Making ATP. Proc. Natl. Acad. Sci. **101**, 16539–16546 (2005)
63. Walz, D., Caplan, S.R.: Energy coupling and thermokinetic balancing in enzyme kinetics—microscopic reversibility and detailed balance revisited. Cell Biophys. **12**, 13–28 (1988)
64. Walz, D.: Biothermokinetics of processes and energy conversion. Biochim. Biophys. Acta **1019**, 171–224 (1990)